10

Bio-Inspired Synthesis of Electrode Materials for Lithium Rechargeable Batteries

Kisuk Kang and Sung-Wook Kim
Seoul National University,
Republic of Korea

1. Introduction

Human history has been made through endless challenges, searching for universal truths of nature. Sometimes, nature becomes a crucial barrier that human beings should overcome, however, repeatedly, it inspires us to make progress in science and results in a better life. Nature always provides pointers in developing technologies; emulating nature serves as a very helpful methodology for such development (Bensaude-Vincent et al., 2002). Figure 1 shows some examples of creations that were invented through the emulation of nature. Especially, living organisms are excellent teachers whose metabolism, vital activity, and growth present novel synthetic routes for the formation of organic (or inorganic) biomaterials (Sanchez et al., 2005). The study of on the biomaterials, highly ordered forms of molecules in a biological system with complex nanostructures, has opened up a new era for fabricating nanomaterials through the emulation of biological processes (Dickerson et al., 2008).

This chapter briefly introduces the bio-inspired synthetic routes of nanostructured electrode materials for lithium (Li) rechargeable batteries using biomaterials as structural templates. Various biomaterials have been synthesized both naturally, *i.e.*, inside living bodies (*in vivo)*, and intentionally in the laboratory (*in vitro)*, (Sanchez et al., 2005; Dickerson et al., 2008). One can synthesize biomaterials that possess unique nanostructures without much difficulty. By controlling the synthesis conditions, the nanostructure of biomaterials can be varied from a simple 0-D structure to complex 3-D structures (Lv et al., 2008). The unique nanostructures of the biomaterials can be applied to various research fields, including not only bio-applications but also non-bio-applications such as semiconductors, display devices, catalysts, and energy conversion/storage devices, by hybridizing them with various functional materials at the nanoscale (Katz et al., 2004; Su et al., 2008; Li et al., 2009). As the minimizing of a material's dimension in a certain shape often provides distinctive material properties due to a large surface-to-volume ratio, geometry, and/or quantum effects, This could lead to breakthroughs in overcoming the limitations of conventional bulk materials (Moriarty, 2001). Thus, the hybridization of nanostructured biomaterials with functional materials frequently offers improved material properties under simple nanofabrication principles.

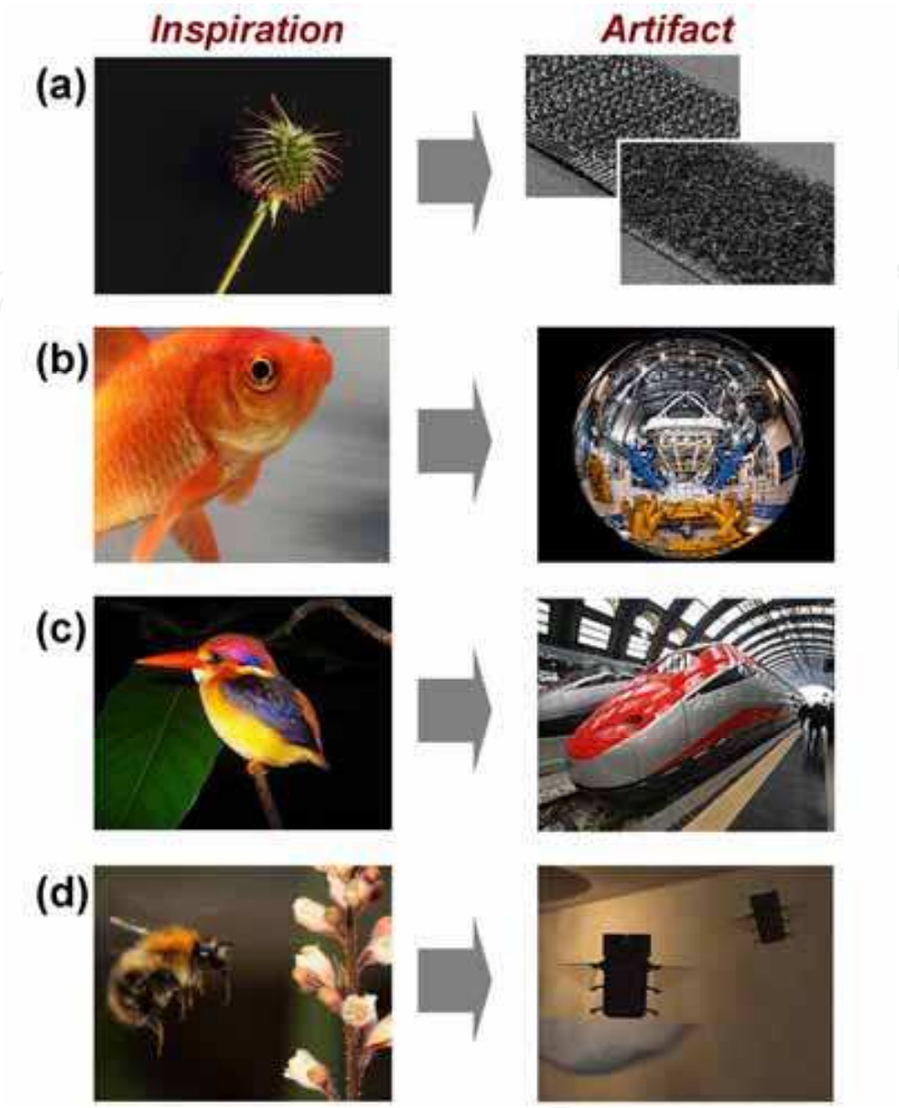

Fig. 1. Photographs of creations inspired by nature: (a) thistles (left) and Velcro® hooks and loops (right), (b) eye of fishes (left) and a fisheye lens (right), (c) kingfisher (left) and bullet trains (right), and (d) bumble bee (left) and micro air vehicle (right). All images were obtained from http://en.wikipedia.org/.

The (Li) rechargeable battery is the leading candidate for large scale energy storage devices due to its high specific capacity, high operation voltage, and thus, high energy density (Tarascon & Armand, 2001). Although the (Li) rechargeable battery has been used most widely as an energy storage system for small portable devices such as lap-top computers and mobile phones, its electrochemical performance is not sufficient to power larger scale energy storage systems such as electric vehicles and load-leveling systems (Kang et al., 2007). In this respect, investigating nanostructured electrode materials has become essential because improvements in electrochemical performance, such as higher specific capacity, higher rate capability, and better cyclability, are expected in this dimension. The nanoscale dimension offers some advantages to the electrochemical performance because of the large

surface area contacting electrolyte, short (Li) ion diffusion length, and facile strain accommodation induced by volume change (Bruce et al., 2008).

Various synthetic routes have been investigated extensively to synthesize novel nanostructured electrode materials. The use of nanostructured templates is one of the most promising approaches because target nanostructures can be obtained simply from the structural duplication of the nanostructured templates (Cheng et al., 2008). Biomaterials, whose varieties of nanostructures are easily obtained by simple control of the synthesis conditions, are considered useful structural templates for nanofabrication (Cui et al., 2010). Also, their surface groups can offer possible nucleation sites for the growth of electrode materials (Ryu et al., 2010a). Nanostructured electrode materials based on biomaterial templates can show improved electrochemical performance compared with that of bulk materials, and their fabrication processes are often more environmentally friendly compared with other methods of preparing nanomaterials.

2. Biomaterials

In living organisms, biomaterials are produced from interpreting the genetic information in nucleic acids such as deoxyribonucleic acids (DNAs) and ribonucleic acids (RNAs). Genetic expression produces proteins, cells, tissues, organs, and finally, bodies. One interesting feature of biomaterials is that they are constructed spontaneously by self-assembly. The term 'self-assembly' refers to the organization of highly ordered nanostructures from disordered components through spontaneous non-covalent interactions between the components under specific conditions without any external driving forces (Reches & Gazit, 2006). When specific condition for self-assembly are satisfied, the components, or building blocks, start to create the nanostructure by themselves, forming various complex nanoarchitectures. Thus, self-assembly is a useful way to fabricate nanostructured materials. The self-assembly Phenomenon frequently occurs naturally in biological systems, forming complex nano-patterned structures (Fraden & Kamien, 2000).

For the past several decades, many research efforts have been focused intensively on the synthesis of biomaterials in the laboratory and on using them to develop conventional bio-applications such as tissue regeneration and artificial organs (Geise et al., 2006). Figure 2 illustrates various shapes of self-assembled biomaterials formed naturally and artificially. They exhibit exclusive structures from nanoscale to macroscale (Brachmann & Cagan, 2003; Ryu & Park, 2008; Xia et al., 2004).

Recently, it has been widely demonstrated that self-assembled biomaterials can serve as structural motifs for non-biological nanostructured materials (Sanchez et al., 2005). Biomaterials are composed of organic materials that contain various functional groups, so their acidities and polarities at the surface can provide possible adsorption sites for precursors of the target nanostructured materials. When the adsorbed precursors react exclusively on the surface to form the target materials, the complex shapes of the biomaterials are duplicated generating isostructural target materials. Some examples of duplicated nanomaterials are presented in Figure 3 (Zhou et al., 2007; Zhang et al., 2010).

Nanomaterials can fully or partially cover the surface of the biomaterials, forming nanoarchitecture similar to that of the template. The duplications of the nanostructure of the biomaterials offers new possibilities for biomaterials in a broad range of research fields beyond the conventional bio-applications by enabling the synthesis of various functional materials in complex forms.

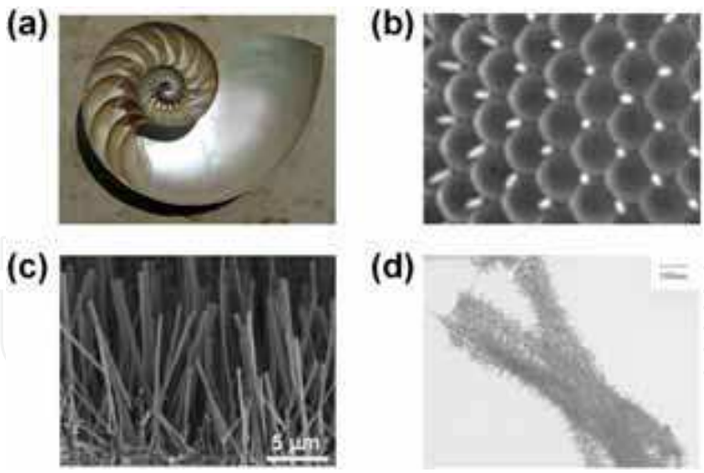

Fig. 2. Photographs of naturally (a-b) and artificially (c-d) self-assembled biomaterials: (a) shell of nautilus (http://en.wikipedia.org/), (b) hexagonal array of eye of *drosophilia* (Brachmann & Cagan, 2003), (c) well-aligned peptide nanowires (Ryu & Park, 2008), and (d) polyaniline-naphthol blue black nanotubes (Xia et al., 2004).

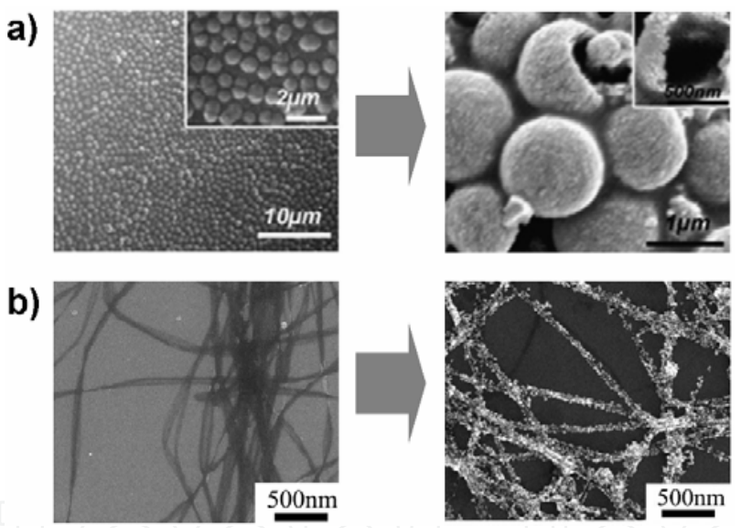

Fig. 3. Nanomaterials fabricated using biomaterials as structural templates: (a) *Str. theromophilus* (left) and ZnO hollow nanospheres fabricated using *Str. theromophilus* as the structural template (right) (Zhou et al., 2007) and (b) bacteria-cellulose nanofibers (left) and Au-bacterial-cellulose nanocomposite (right) (Zhang et al., 2010).

In this respect, the structural control of the biomaterial itself becomes an important technical issue. Artificially self-assembled biomaterials can display various nanostructures depending on the self-assembly conditions. Because the self-assembly is derived from the complicated combination of non-covalent interactions including hydrogen bonds, electrostatic interactions, hydrophobic interactions, and van der Waals interactions between the building blocks and environment, the morphology of biomaterials is significantly affected by the local environment. For example, Figure 4 illustrates a series of nanostructures of a self-assembled aromatic dipeptide, which were produced by

controlling the dissolving solvents (Han et al., 2008). During the process of dissolving and cooling diphenylalanine (NH_2-Phe-Phe-COOH) in H_2O, CH_3OH, C_2H_5OH, or CH_2Cl_2, the diphenylalanine self-assembled into a nanotube shape in H_2O (Figure 4(a)), nanoribbon shape in CH_3OH and C_2H_5OH (Figure 4(b-c)), and a nanoribbon/nanowire shape in CH_2Cl_2 (Figure 4(d)). The solvent polarity affects the force balance between the non-covalent interaction, resulting in various nanostructures obtained with different solvents. If one can prepare the self-assembled biomaterial with precise control of the specific nanostructure, from a simple 0-D to a complex 3-D structure, it would be a very attractive template for the nanostructured functional material. So far, naturally structured biomaterials have been used frequently as templates, and thus, their structural duplications have been studied extensively in research fields where nanostructured materials are required. However, despite the extensive research efforts to control the morphology of biomaterials, further studies are needed to fabricate self-assembled biomaterials with specific shapes.

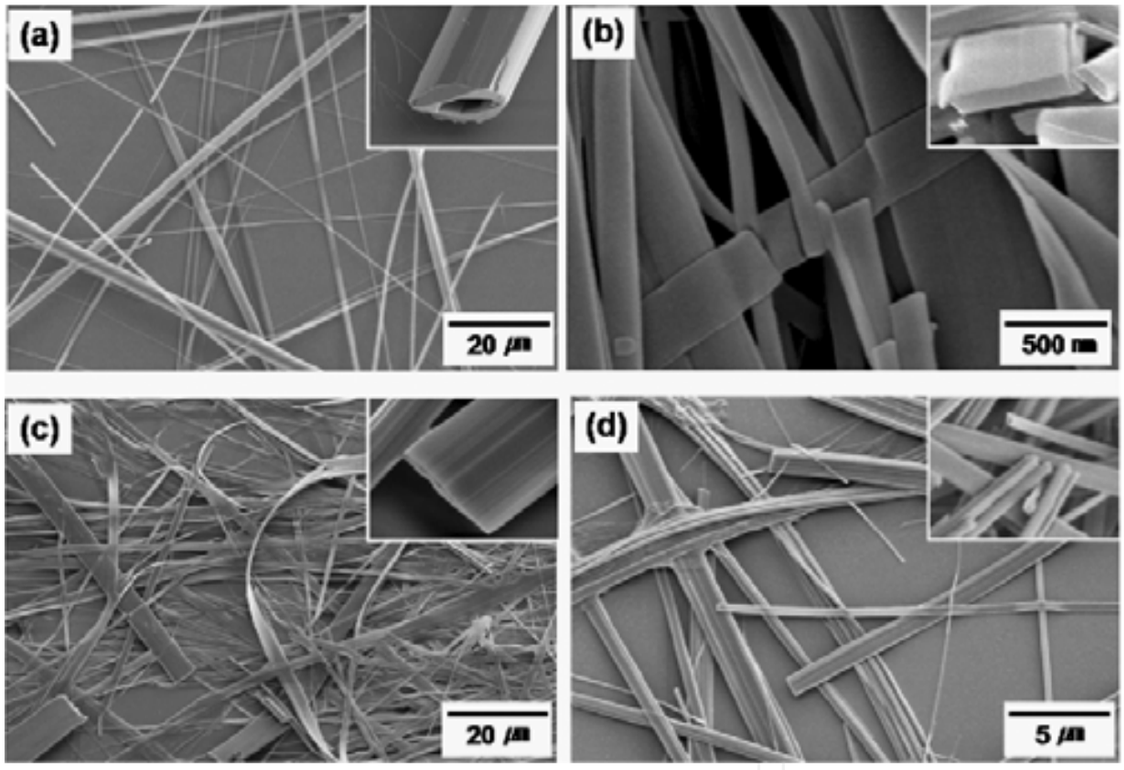

Fig. 4. Morphology of diverse nanostructures of the peptide formed in various solvents: (a) nanotubes formed in H_2O, (b) nanoribbons in CH_3OH, (c) nanoribbons in C_2H_5OH, and (d) nanoribbons and nanowires formed in CH_2Cl_2 (Han et al., 2008).

3. Bio-inspired synthesis of materials for lithium rechargeable batteries

Recently, researchers have tried to find a way to combine biomaterials as a nano-sized structural template with a functional material with the hope that the nanoscale dimension and morphology can improve performance of the material. Among various functional materials under consideration, materials for energy storage/conversion devices attract

much interest because energy problems, such as exhaust and CO_2 emissions of fossil fuels, have become severe (Tarascon et al., 2001). Nanostructured electrode materials for Li rechargeable batteries offer improved electrochemical activity, resulting in enhanced battery performance. However, the realization of the expected nanostructure, *i.e.* morphology and dimension, requires further investigation of the synthetic routes. The bio-inspired synthesis of nanostructured electrode materials can be a useful approach because surface coating onto the nanostructure biomaterials produces materials conformally (Sanchez et al, 2005). When one can control the nanostructure of biomaterials by adjusting the self-assembly conditions, it is easy to synthesize the nanostructured electrode materials with the intended morphology and dimension.

The various synthetic routes for the bio-inspired synthesis of nanostructured electrode materials are described in this section. Potential electrode materials, such as the Co_3O_4 anode, TiO_2 anode, and amorphous $FePO_4$ cathode, could be fabricated onto biomaterials by wet-chemistry or vapor deposition processes. Because the biomaterials generally possess polarity or various functional groups on the surface, many chemical species such as ions and molecules can be adsorbed on the surface, reacting into the electrode materials. Organic-inorganic hybrid materials, ensembles of the organic biomaterial templates and the inorganic electrode materials, can be adopted as electrode materials. Additionally, removing the biomaterial template in the hybrid materials leaves hollow-structured materials with superior electrochemical performances as the electrode.

3.1 Virus-based hybrid electrode materials

Enhanced electrochemical activity in the nanoscale dimension is an important reason for challenges to apply bio-inspired synthesis to Li rechargeable battery materials, due to its precise structure controllability. Another reason is the soft, flexible, and self-standing properties of the biomaterials. Increasing demands for portable, wearable, and stretchable electronic devices have created a need for flexible batteries, which can only be realized by using flexible electrode materials. As such, biomaterials are considered as excellent supporting materials for electrode materials. Biomaterials such as viruses and peptides are promising templates for the nanostructured electrode materials due to their capabilities to form unique nanostructures uniformly over a large area. When the electrode materials precipitate onto the surface of the biomaterials, forming organic-inorganic hybrid materials, it is expected that the hybrid materials can exhibit electrochemical activity combined with flexibility.

Viruses are kind of parasitic pathogens inside living organisms that replicate themselves. Their genetic information is stored in either DNA or RNA. They can replicate only inside the infected cells of the hosts because they do not have any organs for metabolism and energy production. Since the first observation of tobacco mosaic virus in 1892, various viruses have been reported inside all types of living organisms, from small protozoa to large mammals. Among them, the M13 virus is one of the most frequently investigated viruses for nanotechnology (Lee et al., 2003). The M13 virus, shown in Figure 5, possesses a wire-like anisotropic structure approximately 6.5 nm in diameter and 880 nm in length (Nam et al., 2004). The M13 virus particle is composed of circular single-stranded DNA encapsulated by a major coat protein (p8) and capped by minor coat proteins (p3, p6, p7, and p9) at the end of the virus.

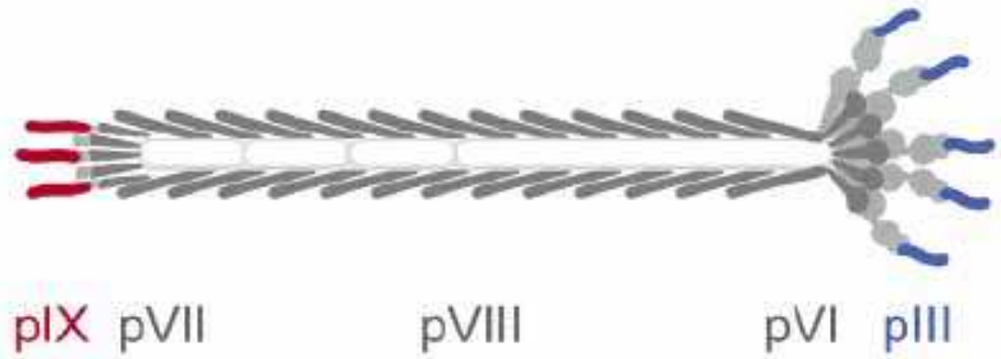

Fig. 5. Schematic representation of a genetically modified M13 virus (Nam et al., 2004).

Hybridizing the M13 virus with functional inorganic materials is possible through modification of the major and/or minor coat proteins because the modified proteins provide nucleation sites for the inorganic materials. The configuration of the proteins is determined by the genetic information. Hence, modifying the genetic information in DNA creates modified proteins and thereby the modified M13 viruses. Figure 6(a) briefly describes the hybridization process of ZnS-M13 virus with genetic modification. The major coat protein, p8, is modified to induce the nucleation of ZnS nanoparticles. The configuration of the protein is determined by considering the compatibility with ZnS nanoparticle growth. In this case, the A7 (Cys-Asn-Asn-Pro-Met-His-Gln-Asn-Cys) peptide strongly adsorbs Zn^{2+} ions. The modified M13 virus is stored in $ZnCl_2$ solution, and then Na_2S solution is introduced to synthesize the ZnS-virus hybrid material. As a result, ZnS nanoparticles cover the surface of the virus conformally (Figure 6(b-c)).

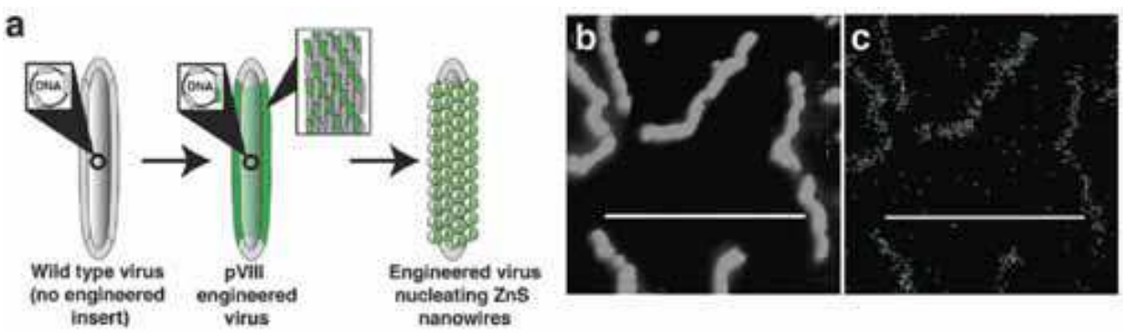

Fig. 6. (a) Schematic diagram of the hybridization process of ZnS-virus nanowire through the genetic modification of p7 proteins, (b) STEM images of the synthesized ZnS-virus nanowire, and (c) EDS mapping of S of the same sample. (Scale bars: 800 nm) (Mao et al., 2003).

As the M13 viruses are able to bind inorganic materials through the genetic modification, it is possible to use the modified M13 viruses as biotemplates for the nanostructured materials used in Li rechargeable battery electrodes. Figure 7 represents the M13 virus genetically modified to bind amorphous $FePO_4$ cathode material and highly conductive carbon nanotubes (CNTs) (Lee et al., 2009). Amorphous $FePO_4$ is an attractive cathode material due to its high specific capacity and safety originating from the strong $(PO_4)^{3-}$ covalent bond, but its poor electronic/Li-ionic conduction precludes further investigation

(Okada et al., 2005). Therefore, developing nano-sized amorphous $FePO_4$ with a highly conductive agent is essential for the high performance Li rechargeable battery. The modified M13 virus enables the formation of amorphous $FePO_4$ nanoparticles at the p8 proteins and, at the same time, combines with the CNT at the p3 proteins as the result of genetic modification of the p8 and p3 genes.

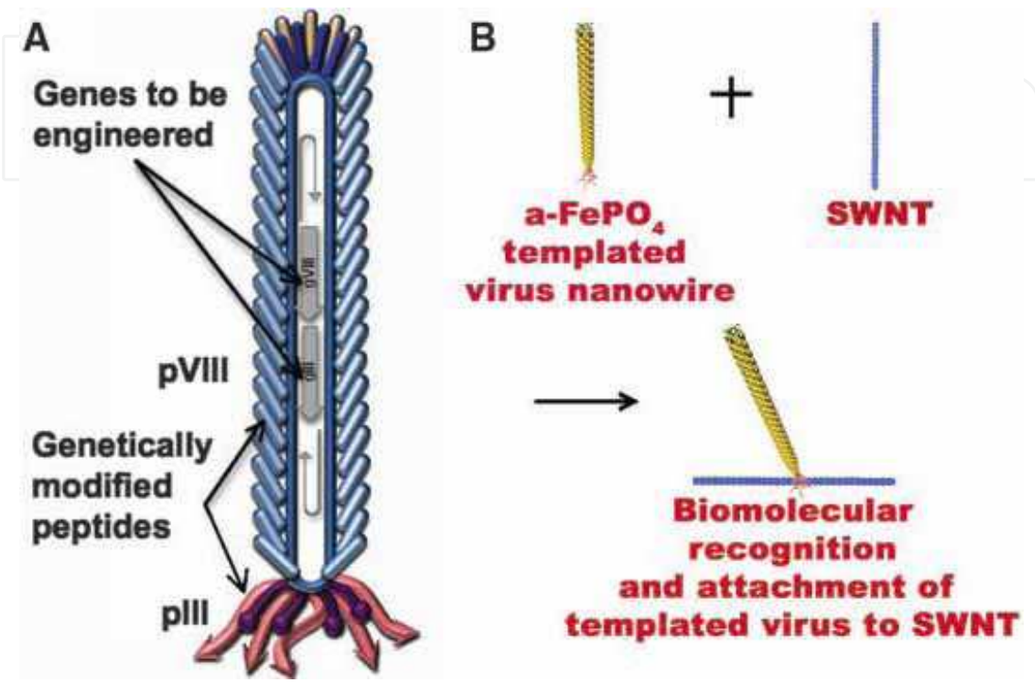

Fig. 7. Schematic illustration presenting the process of the virus-amorphous $FePO_4$-CNT hybrid material for a high-power Li rechargeable battery: (a) multifunctional M13 virus obtained through genetic modification and (b) the hybridization process with the modified M13 virus (Lee et al., 2009).

The hybrid nanowire is synthesized by the following sequence: (i) genetic modification of the M13 virus to bind amorphous $FePO_4$ at p8 proteins and CNTs at p3 proteins, (ii) Au nanoparticle loading onto the virus, (iii) formation of amorphous $FePO_4$ onto the Au-loaded virus template to enhance electrical conduction, and finally, (iv) reacting the virus-amorphous FePO4 nanowires with CNT suspensions with surfactant. Because the modified p8 proteins contain extra carboxyl acid groups, metallic cations can interact readily with the virus. The modified p3 proteins have a high affinity for CNTs; thus, the virus-amorphous $FePO_4$ nanowire can bind CNTs to form the hybrid nanowire. The synthesized hybrid material composed of virus template-amorphous $FePO_4$ electrode materials-CNT conductive agent is shown in Figure 8 (Lee et al., 2009). The hybrid material possesses a complex network structure of individual nanowires, which has the same morphology as that of the virus template without any hybridization process. The diameter of amorphous $FePO_4$ nanoparticles is approximately 10-20 nm, and that of CNTs is approximately 4-5 nm. Amorphous $FePO_4$ and CNTs are well connected each other, as shown Figure 8(e), indicating that electrons are rapidly supplied to the amorphous $FePO_4$ cathode through the CNT networks.

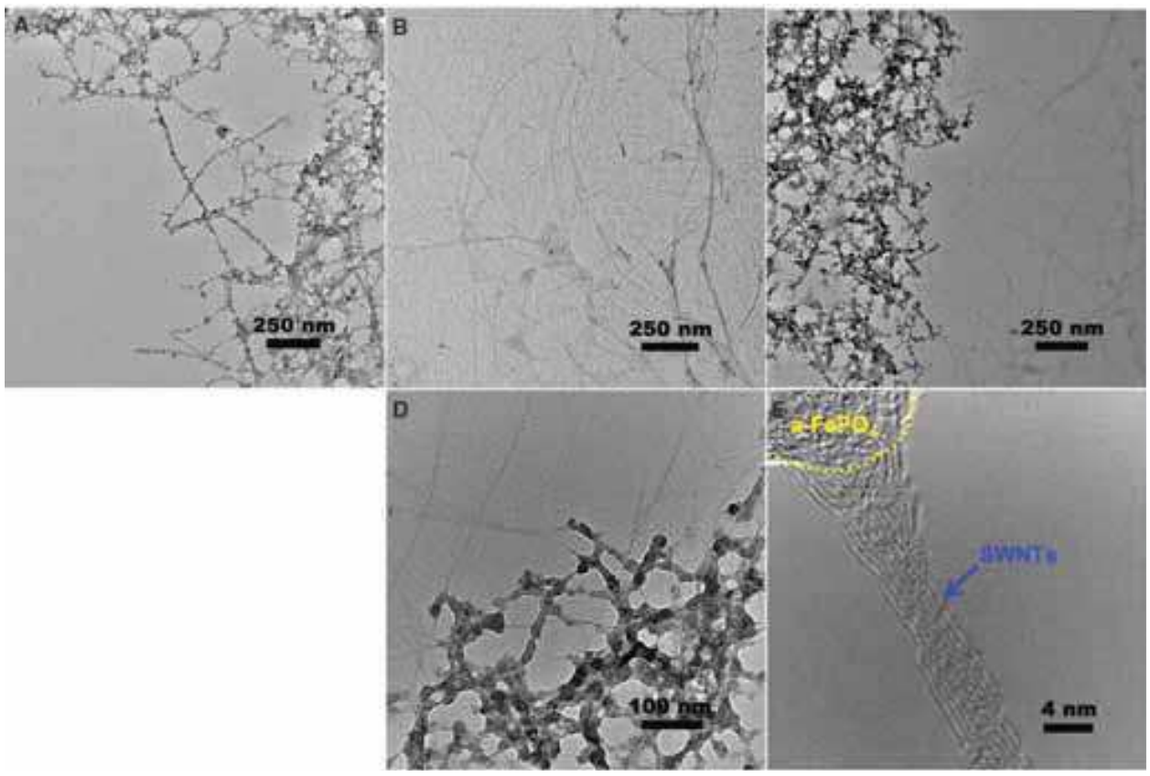

Fig. 8. Nanostructure of synthesized hybrid nanowires: (a) virus-amorphous $FePO_4$ hybrid nanowires without CNTs, (b) bare CNTs, and (c-e) virus-amorphous $FePO_4$-CNT hybrid nanowires at different resolutions (Lee et al., 2009).

The simultaneous supply of Li ions and electrons in/outside of active electrode materials is essential for the operation of the Li rechargeable battery. It is obvious that a faster supply results in higher performance during operation. The dimension shrinkage of electrochemically active material, *i.e.*, amorphous $FePO_4$, reduces the distance for Li-ion penetration. The CNT networks continuously supply electrons to the active material. Hence, superior electrochemical performance is accomplished in the virus-amorphous $FePO_4$-CNT hybrid nanowires, as depicted in Figure 9 (Lee et al., 2009). Figure 9 compares the electrochemical properties of three types of hybrid nanowires; which are virus-amorphous $FePO_4$ hybrid nanowires without CNTs (E4), virus-amorphous $FePO_4$-CNT hybrid nanowires with moderate binding affinity to CNTs (EC#1), and those with strong binding affinity to CNTs (EC#2). EC#1 and EC#2 display higher specific capacity at every current rate compared with E4, indicating that the CNT networks sufficiently provide electrons during the electrochemical reaction. Especially, EC#2 exhibits superb electrochemical performance. The specific capacity of EC#2 at a current of C/10 (1C = 178 mA g^{-1}) is approximately 170 mAh g^{-1}, which is comparable to that of a theoretical one. Its high capacity is maintained at higher current rates, indicating that the hybrid nanowires are promising candidates for high-power applications. The specific capacity of EC#2 at 10C is as high as 130 mAh g^{-1}. Additionally, all samples show excellent cycle retention up to 50 cycles, indicating that the hybrid nanowires remain stable upon electrochemical cycling.

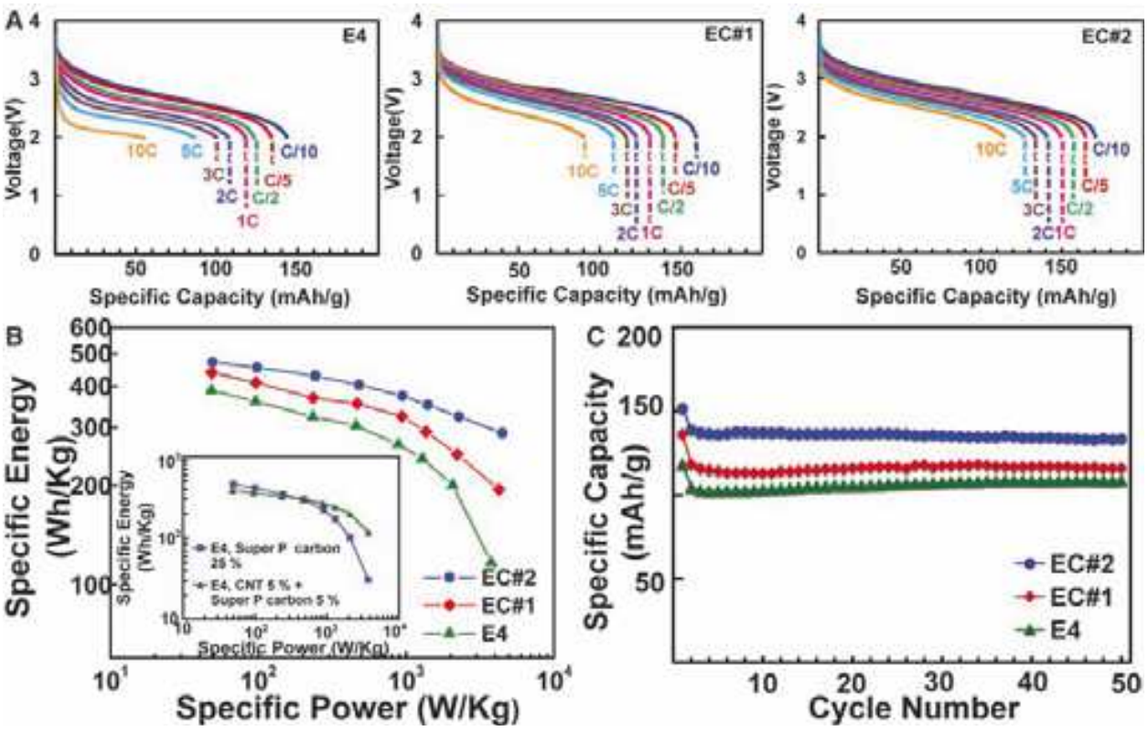

Fig. 9. Electrochemical performance of hybrid nanowires based on multifunctional M13 virus templates: (a) discharge profiles of E4 (virus-amorphous $FePO_4$ nanowires), EC#1 (virus-amorphous $FePO_4$-CNT nanowires with moderate affinity for CNTs), and EC#2 (virus-amorphous $FePO_4$-CNT nanowires with strong affinity for CNTs) at current rates from C/10 to 10C, (b) Ragone plots of the hybrid nanowires (inset: Ragone plot of E4 as a function of carton contents), and (c) capacity depending on the number of cycles at a current rate of 1C for 50 cycles (Lee et al., 2009).

The same strategy of a modified virus as a structural template could be adoptable for other kinds of electrode materials. Co_3O_4 is one of the most promising anode materials for the Li rechargeable battery due to its high specific capacity (~890 mAh g^{-1}) through a conversion reaction (Kang et al., 2005). Although the Li_2O phase, a product of the conversion reaction of Co_3O_4, is electrochemically inactive, it becomes electrochemically active when the dimension of Li_2O is reduced to nanoscale. Thus, the nanofabrication of Co_3O_4, the mother phase of Li_2O, is essential for the highly active Co_3O_4 anode (Li et al., 2008). The genetically modified M13 virus could define the nanostructure of Co_3O_4. Figure 10(a) simply illustrates the modification of the M13 virus (Nam et al., 2006). The surrounding p8 proteins are modified to two types: one contains a Co nucleating motif, and the other contains Au binding motif. The virus-Au-Co_3O_4 hybrid nanowires are fabricated through an Au-binding followed by Co_3O_4 nucleation and growth. Viruses that do not contain the Au binding motif cannot bind Au nanoparticles at all. Uniform Au nanoparticles (~5 nm in diameter) are finely dispersed in the hybrid nanowires, as shown in Figure 10(b-c) (Nam et al., 2006). The hybrid nanowires show excellent electrochemical properties due to the improved electrochemical activity of the conversion reaction in the nanoscale dimension. The Au-containing nanowires exhibit better performance, indicating that Au nanoparticles further improve the electrochemical activity. This is due to the increased electronic conduction, or catalytic effect

of the Au nanoparticles. The increase in the current density at CV measurement shown in Figure 10(e) indicates that the incorporating of Au nanoparticles increases the reaction rate of the Co_3O_4 anode (Nam et al., 2006).

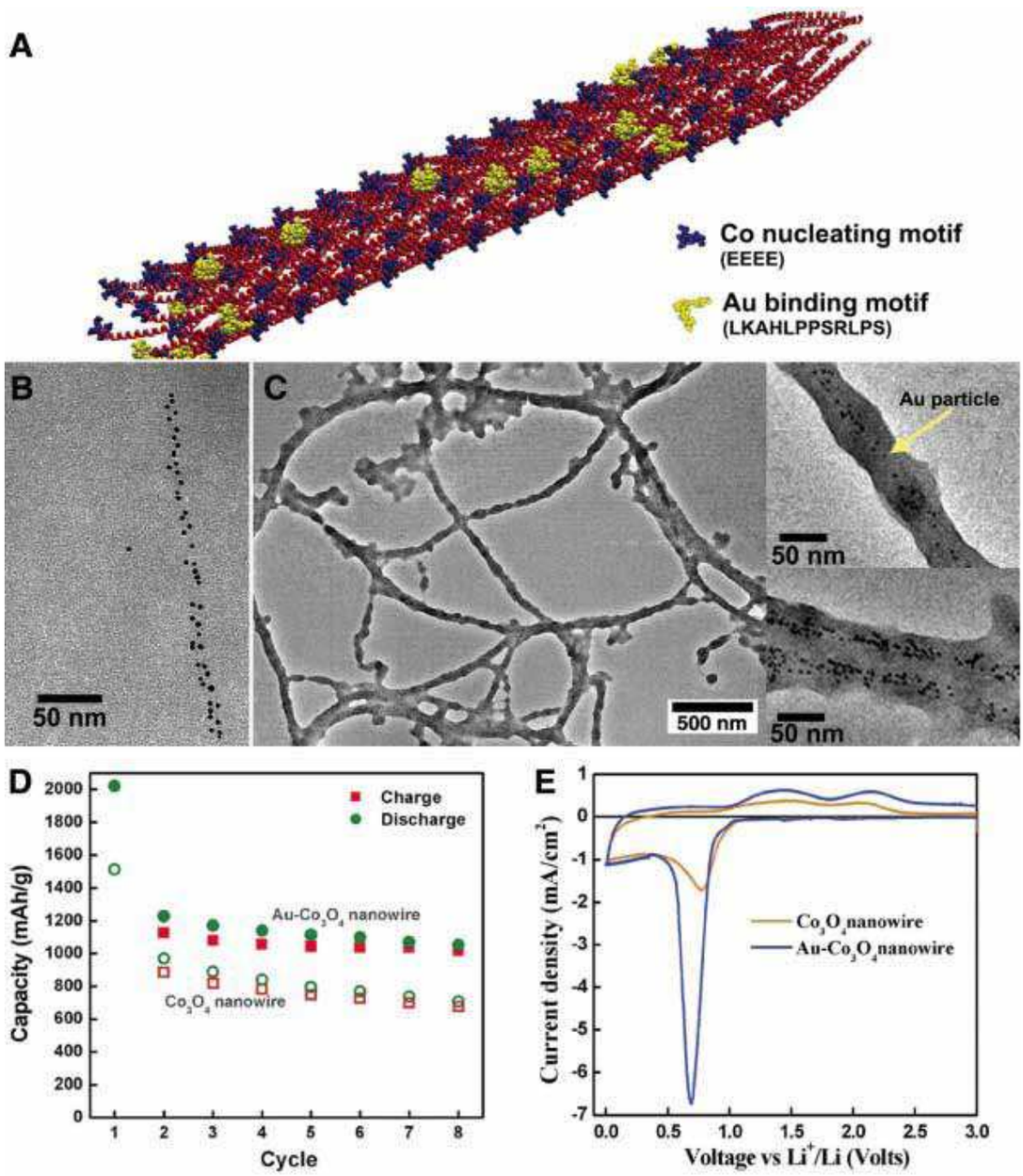

Fig. 10. Nanostructures and electrochemical properties of the virus-Au-Co_3O_4 hybrid nanowires: (a) schematic visualization of the modified M13 virus with both a Co-nucleating motif (blue) and an Au-binding motif (yellow), (b) the virus-Au hybrid nanowire before Co_3O_4 growth, (c) the virus-Au-Co_3O_4 hybrid nanowire, (d) specific capacity depending on the number of cycles of the hybrid nanowires with and without Au at a current of C/26.5 for 8 cycles, and (e) CV curves of the nanowires with and without Au at a scan rate of 0.3 mV s^{-1} (Nam et al., 2006).

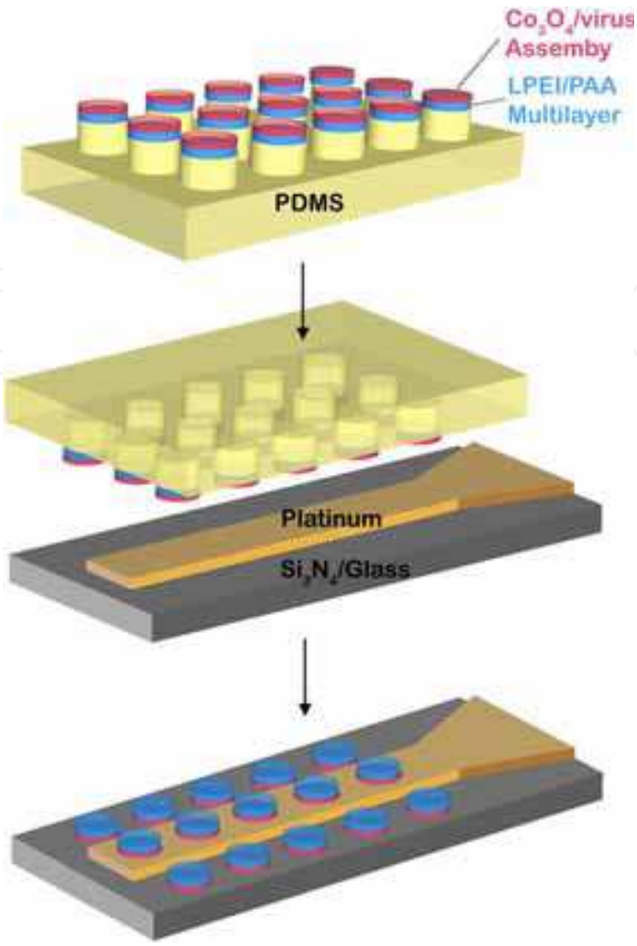

Fig. 11. Schematic diagram of the fabrication procedure for a virus based microbattery electrode (Nam et al., 2008).

When a virus is genetically modified to have high affinity for a certain substrate, the virus can be assembled with the substrate without difficulty. This enables the growth of the virus in any place with the expected shapes by surface modification using a thin layer of the substrate having high affinity to the virus. This means that the virus-based synthesis could be applied widely in micro/nano-patterned devices. In this respect, microbattery fabrication with modified virus has been investigated, as illustrated in Figure 11 (Nam et al., 2008). As the modified M13 virus is known to be easily assembled onto polyelectrolyte multilayers, a linear-polyethylenimine (LPEI)/polyacrylic acid (PAA) multilayer is prepared as a solid electrolyte as well as a separator on the patterned polydimethylsiloxane (PDMS) substrate. The positive LPEI and negative PAA layers electrostatically combine to form a multilayer film through a layer-by-layer deposition technique. The modified virus is grown onto the film by dropcasting, and then Co_3O_4 is nucleated on the virus template. Figure 12 shows AFM images of the fabricated virus-Co_3O_4 anode onto the multilayer film (Nam et al., 2008). The virus tends to form a 2-D liquid crystalline assembly as a result of the interaction between the viruses and LPEI/PAA multilayers. Such a 2-D nanostructure confers an advantage upon the microbattery due to its high packing density. Finally, the virus-Co_3O_4 anode/multilayer

film structure is transferred to Pt current collectors by a stamping process, and the electrode is electrochemically characterized, as shown in Figure 13 (Nam et al., 2008). The electrode can store and release Li-ions reversibly, demonstrating that the virus assembly represents an adequate process for fabricating microbattery electrodes.

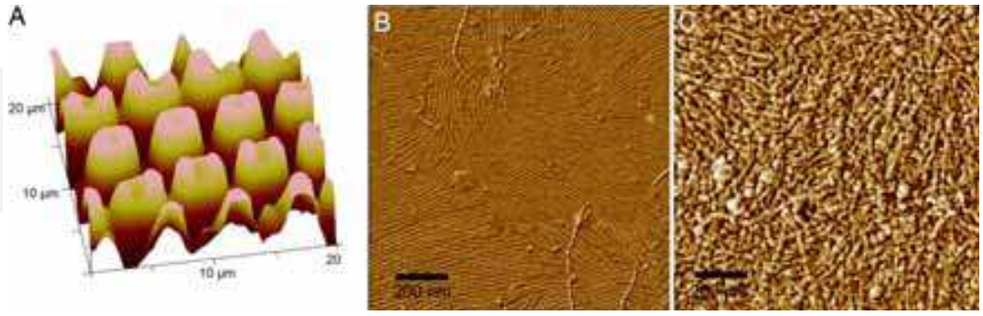

Fig. 12. AFM images of the virus-based microbattery: (a) height image of stacks of the virus-Co_3O_4/(LPEI/PAA) multilayer/PDMS electrode, and phase image of the virus assembly onto the multilayer (b) before and (c) after the nucleation of Co_3O_4 (Nam et al., 2008).

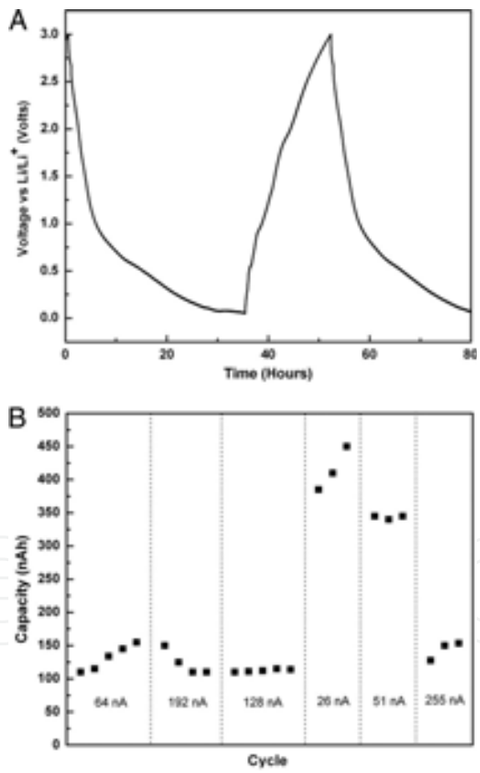

Fig. 13. Electrochemical properties of the virus based microbattery electrode: (a) charge-discharge profiles at a current rate of 26 nA in the voltage range of 0.01-3 V and (b) capacity depending on current rate, from 26 nA to 255 nA (Nam et al., 2008).

The self-assembled biomaterials are flexible and self-standing, even in the macroscopic dimension. LPEI/PAA multilayers (just described above) could be fabricated as flexible, transparent, and self-standing films. When the modified M13 virus is assembled onto the

surface of the film (Figure 14(a-b)), Co_3O_4 anode material can be grown through the virus template (Nam et al., 2006). The self-standing film with the anode material can be rolled and bent without any crack propagations as shown in Figure 14(c) (Nam et al., 2006). Figure 14(d) shows that the virus-Co_3O_4 anode assembled on the multilayer film exhibits high specific capacity, even at high current rates (Nam et al., 2006). This result indicates that the genetic modification of the virus to assemble onto the self-standing polymer film is a promising strategy for investigating flexible Li rechargeable battery electrodes.

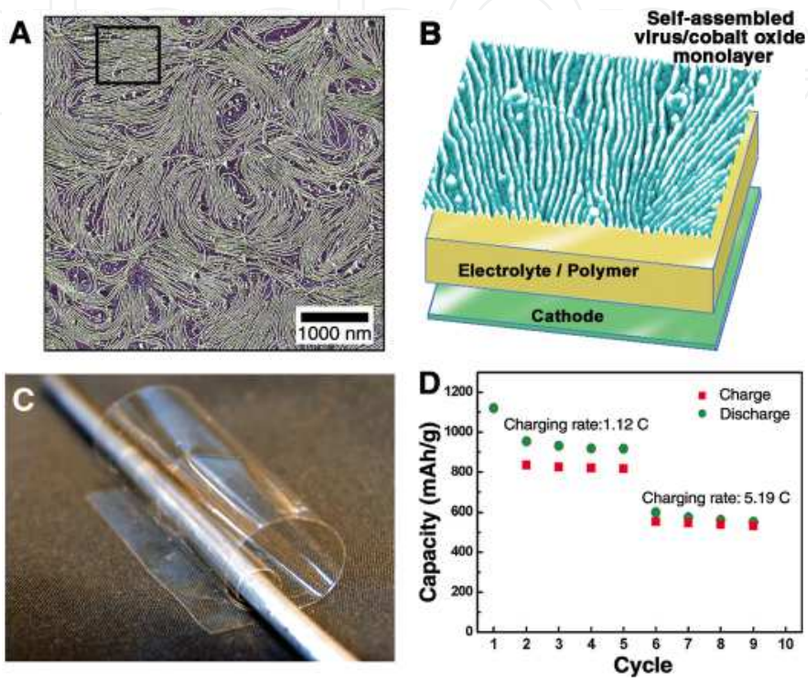

Fig. 14. Self-standing and flexible electrode film based on the virus-Co_3O_4 nanowires: (a-b) phase-mode AFM image of the virus-Co_3O_4 nanowires, (c) photograph of the electrode film composed of virus-Co_3O_4 on a LPEI/PAA multilayer with excellent flexibility, and (d) electrochemical property of the virus-Co_3O_4 anode at current rates of 1.12C and 5.19C. (Nam et al., 2006).

The virus, which can be genetically modified to change the proteins to control its affinity for other materials, provides a promising approach to fabricating the nanostructured electrode materials for Li rechargeable batteries. The improved affinity offers potential nucleation sites for not only various electrode materials (*e.g.*, Co_3O_4 and amorphous $FePO_4$) but also highly conductive materials (*e.g.*, CNT and noble metals such as Au, Ag, and etc). The virus-based hybrid materials, which contain the electrochemically active nanomaterial with the conductive agent, exhibit superior electrochemical performance for high-power Li rechargeable batteries due to the enhanced Li-ionic and electronic conduction. More interestingly, the genetic modification can control the nanostructures of the virus templates, as depicted in Figure 15 (Nam et al., 2005; Huang et al., 2004). Although virus assembly to simple wire-like virus template is well established, further studies should be undertaken to investigate the control of the shapes of the virus assembly, from simple 0-D to complex 3-D architectures, and their use as structural templates because the electrode performance could be strongly influenced by the nanostructure. When genetic technologies to precisely control

the virus assembly and the affinity for the electrode materials are achieved, the barriers limiting the conventional Li rechargeable battery could be overcome.

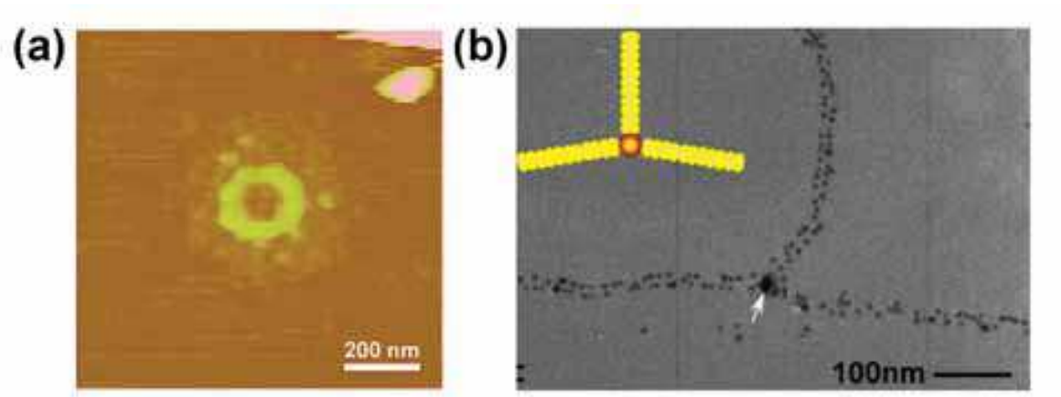

Fig. 15. Various nanostructures of modified viruses: (a) ring-shape (Nam et al., 2005) and (b) Y-shape (Huang et al., 2004).

3.2 Nanotubular electrode materials based on peptide assembly

When a carboxyl group (-COOH) of one amino acid meets an amino group (-NH_2) of another amino acid, the functional groups of each molecule can interact to form a covalent bond (-C(=O)NH-) through a dehydration reaction, as illustrated in Figure 16. This covalent bond is called a 'peptide bond' (Stoker, 2010). The formation of peptide bonds occurs continuously in living organisms to form proteins. Proteins are biological molecules composed of one or more polypeptides, which are long chains linked through number of peptide bonds. Commonly, a peptide is discriminated from a protein in terms of the chain length, *i.e.*, the number of peptide bonds. When the chains are short enough to be synthesized *in vitro*, the molecule is generally called a peptide, but this classification is not always consistent. Peptides are classified by the number of peptide bonds, such as dipeptide, tripeptide, tetrapeptide, and so on. The proteins in the genetically modified viruses possess a high affinity for the electrode materials of Li rechargeable batteries, as described above. Because peptides and proteins are identical in terms of their component species, peptides are also able to provide nucleation and growth sites for various electrode materials. The surface functional groups of the peptides, such as carboxyl groups, are beneficial for coating the electrode materials onto the peptides.

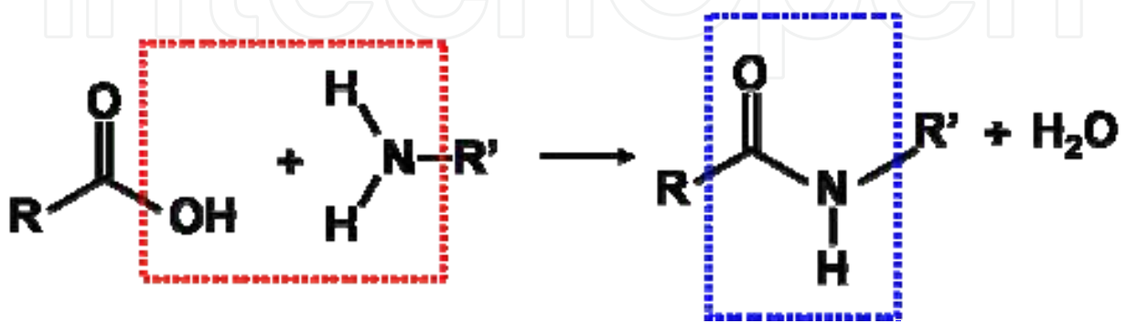

Fig. 16. Formation of a peptide bond between a carboxyl group and an amino group through a dehydration reaction.

The nanostructures of peptides are easily varied by controlling the self-assembly conditions, as shown in Figure 4 (Han et al., 2008). The structural duplication with the electrode materials is achieved by various surface-coating methods, including conventional aqueous solution-based synthesis as well as vacuum vapor deposition . For example, Figure 17 shows hybrid nanowires of diphenylalanine peptide nanowires and Co_3O_4 nanoparticles (Ryu et al., 2010b). Co_3O_4 nanoparticles are formed on the peptide surface by a simple reduction and oxidation process. Although a higher specific capacity is attributed after Co_3O_4 coating (Figure 18), the electrochemical performance of the hybrid nanowires is not sufficiently high, despite the nanoscale nature of Co_3O_4 (Ryu et al., 2010b). The reversible specific capacity of the pure peptide nanowires and the hybrid nanowires is approximately 25 and 80 mAh g^{-1}, respectively. The specific capacity of the hybrid nanowire is very low compared to that of pure Co_3O_4 (890 mAh g^{-1}). This is because the portion of Co_3O_4 nanoparticles in the hybrid is too limited.

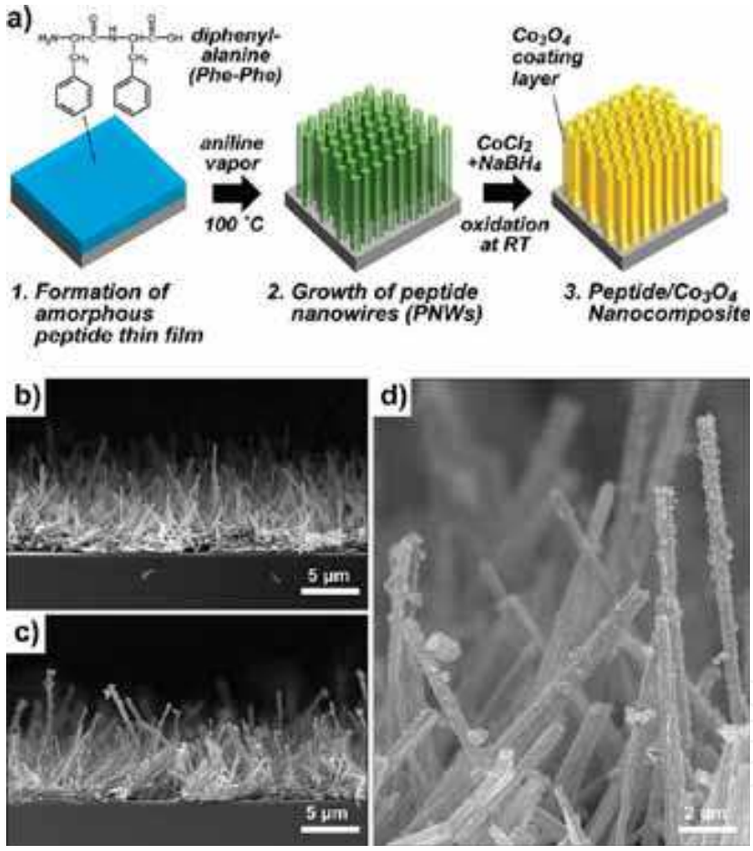

Fig. 17. Diphenlyalanine-Co_3O_4 hybrid nanowires: (a) schematic illustration of the fabrication process of hybrid nanowires and SEM images of (b) the pure peptide nanowires and (c-d) the hybrid nanowires (Ryu et al., 2010b).

When hybrid electrode materials contain electrochemically inactive or less active species to Li ions, their gravimetric and volumetric energy densities decline, as in the case of peptide-Co_3O_4 hybrid nanowires. It is essential to increase the portion of active species, *i.e.*, electrode materials, in the hybrid materials for higher energy-delivery capability. Thus, controlling the portion of the peptide template and the electrode material becomes very important in the

fabrication of peptide-based nanostructured electrode materials. In this respect, removing the peptide template has been suggested to increase the energy-delivery capability (Kim et al., 2009; Ryu et al., 2010b).

The minimized portion of the peptide of the hybrid materials can exhibit a capacity approaching the theoretical capacity of the electrode material. Additionally, the template removal leaves a nanotubular structure of the electrode material, which has advantages over simple nanostructures for battery performance.The unique property of the nanotube is that the structure has surfaces both inside and outside of the tube. The dual-surface system is beneficial for the electrode material because it allows two-directional Li-ion diffusion, twice the contact area to electrolyte, and stress relaxation by the hollow during battery operation.

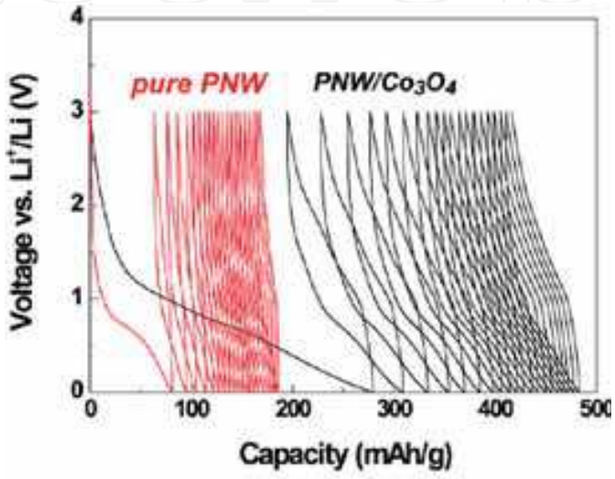

Fig. 18. Discharge-charge profiles of pure peptide nanowires (red) and peptide-Co_3O_4 hybrid nanowires (black) (Ryu et al., 2010b).

The fabrication process for the nanotubular electrode material based on the peptide template is briefly explained in Figure 19 (Kim et al., 2009). After self-assembly of the peptide molecules, the electrode material is coated onto the peptide surface. When the electrode materials fully cover the peptide surface, the peptide template is removed by adequate heat treatment. As a result, only the nanotubular electrode material remains. In this case, a TiO_2 anode is coated onto the peptide template by atomic layer deposition (ALD). ALD is a kind of vapor deposition method that is generally used in fabricating thin films of semiconductor devices (Kim et al., 2008). The self-limited monolayer adsorption, *i.e.*, only chemisorption and not physisorption, of ALD is adoptable for coating the peptide template because the self-limited reaction takes place only at the surface where chemical species for the ALD precursor adsorption site exist (Zhao et al., 2009). The various surface functional groups of the peptide template provide the adsorption sites. This is similar to the adsorption of metal ions in aqueous solution. In ALD, thin-film thickness is controlled digitally by controlling the number of cycles. One cycle is composed of four steps: (i) injection of metal precursor, (ii) Ar purge to remove the residual precursor, (iii) injection of reactant gas, and (iv) another purge (George, 2010). The amount of adsorbed precursors is not varied in ALD because the number of chemisorption sites is identical after the substrate surface is fully covered with the deposited thin film, hence the thin-film thickness is determined by the number of cycles. The digital thickness controllability is beneficial for fabricating a thin film of a specific thickness.

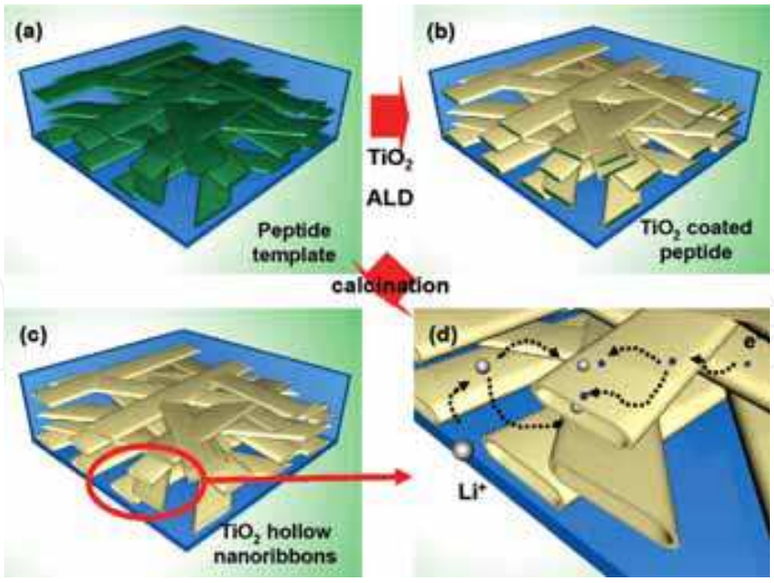

Fig. 19. Schematic illustration of the synthesis process for a network structure of TiO_2 nanotubes based on peptide assembly and ALD: (a) peptide network template, (b) TiO_2 coated peptide network by ALD, (c) TiO_2 nanotube network after removing the peptide template, and (d) Li-ion and electron transports expected in TiO_2 nanotube network structure (Kim et al., 2009).

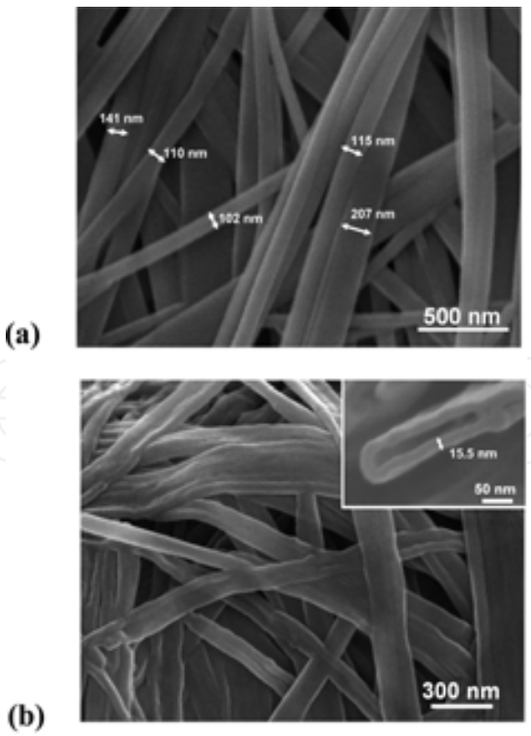

Fig. 20. SEM images of (a) the peptide template and (b) the TiO_2 nanotube network (inset: magnified cross-sectional image of TiO_2 nanotube) (Kim et al., 2009).

Figure 20 represents SEM images of the peptide template and the TiO_2 nanotubes after coating TiO_2 and removing the peptide (Kim et al., 2009). The dimension of the mother phase, the peptide template, is successfully duplicated with slightly larger dimensions forming a continuous thin film on the peptide through ALD. The inset in Figure 20(b) clearly indicates that fabricated TiO_2 is the nanotubular structure, as expected. Such a network structure of TiO_2 nanotubes is expected to exhibit improved kinetics. Facile Li-ionic conduction through the inside and outside of the nanotube and electronic conduction through the interconnected TiO_2 nanotubes seem to be promising for high-power operation.

TiO_2 is known to be an anode material with high safety because the formation of a solid-electrolyte-interphase (SEI) layer, which could trigger heat generation during malfunctioning of the battery, is suppressed due to the relatively high operation voltage window (>1.0 V) (Xu et al., 2008). Nevertheless, its relatively low practical capacity (167.7 mAh g^{-1}) is a significant drawback. The strong Li-Li repulsion restricts Li-ion intercalation more than $Li_{0.5}TiO_2$. It is reported that this is possible in nanoscale due to the surface layer of TiO_2 (<7 nm) (Wagemaker et al., 2007). The discharge-charge profiles of the fabricated nanostructured TiO_2 provided in Figure 21(a) show that Li-ion intercalation of more than $Li_{0.5}TiO_2$ is achieved (Kim et al., 2009). The reversible capacity is approximately 198.3 mAh g^{-1} ($Li_{0.59}TiO_2$) after the initial cycle. The slight initial capacity loss might be attributed to surface defects, which are observed frequently in nanostructured materials. The relatively high first-cycle irreversible capacity can be a general drawback associated with nanostructure electrode materials.

The high specific capacity of the fabricated TiO_2 nanotube network and that of the conventional spherical TiO_2 nanoparticle are compared in Figure 21(b) (Kim et al., 2009). Although the specific capacity of 20-nm TiO_2 nanoparticles is comparable to that of the TiO_2 nanotube network at a low current rate, the TiO_2 nanotube network shows much better high-rate capability due to the improved Li-ionic and electronic conduction, as illustrated in Figure 19(d) (Kim et al., 2009). Furthermore, the TiO_2 nanotube network shows excellent cyclability, as shown in Figure 21(c) (Kim et al., 2009). When Li ions are inserted (or extracted) into (or out of) the host material, a volume change generally occurs, inducing strain on the host material. Repeated Li-ion insertions and extractions can break out a fracture of the host material, resulting in poor cycle stability. Nanotubular structures, which contain hollow space, are believed to accommodate this strain because the volume change is bidirectional, *i.e.*, inward and outward relative to nanotubes. Additionally, the highly ordered network structure enhances the structural stability upon electrochemical cycling. As a result, such a network structure of nanotubes based on peptide assembly is considered to represent a promising strategy for investigating electrode materials with superior electrochemical performance.

Although the nanotube network structures based on ALD onto the peptide assembly are expected to possess excellent electrochemical properties, the relatively high production cost and low precursor efficiency of ALD are demerits for commercialization. In this respect, an aqueous solution-based mineralization technique can be advantageous in fabricating the nanotube network structure. Figure 22(a) simply describes the process for the synthesis of the network structure based on the sequential adsorption method using aqueous solution (Ryu et al. 2010a). An amorphous $FePO_4$ cathode is chosen as a coating material because Fe^{3+} and PO_4^{3-} ions are dissolved readily in H_2O. The conformal thin-film coating in ALD is achieved by separate injections of the metal precursor and the reactant gas. Similarly, separate injections of an aqueous solution of Fe^{3+} and another solution of PO_4^{3-} are believed

to result in conformal coating of amorphous $FePO_4$. Peptide molecules (Fmoc-diphenylalanine; Figure 22(b)), are assembled into the network in H_2O, as depicted in Figure 22(c-d) (Ryu et al. 2010a). The peptide hydrogel is formed in a filtration apparatus, and then the solution of Fe^{3+} is injected and stored inside the apparatus for adsorption of Fe^{3+} ions onto the peptide surface. The solution containing Fe^{3+} is removed by filtration, and then the solution containing PO_4^{3-} is injected, stored, and filtered. The sequential injection of two solutions is repeated to obtain a suitable amount of coated $FePO_4$. This process is very similar to that of the ALD discussed with regard to the TiO_2 nanotube network.

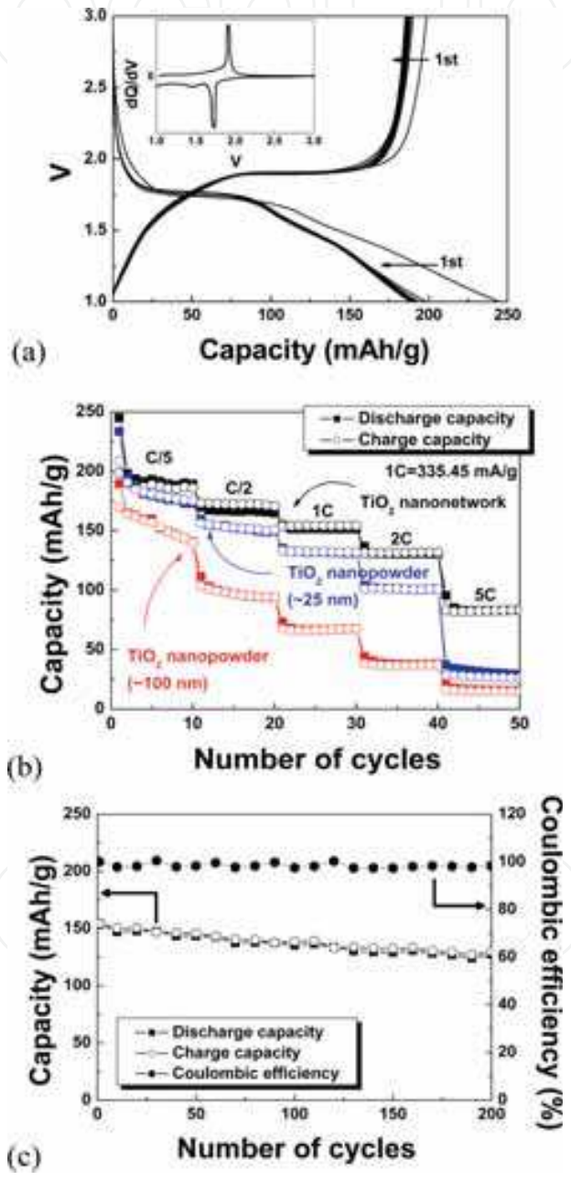

Fig. 21. Electrochemical properties of a TiO_2 nanotube network: (a) discharge-charge profiles at a current rate of C/5 (inset: differential capacity curve at the first cycle), (b) high rate capability compared with conventional TiO_2 nanoparticles, and (c) capacity retention and Coulombic efficiency at a current rate of 1C (1C = 335.45 mAh g-1) (Kim et al., 2009).

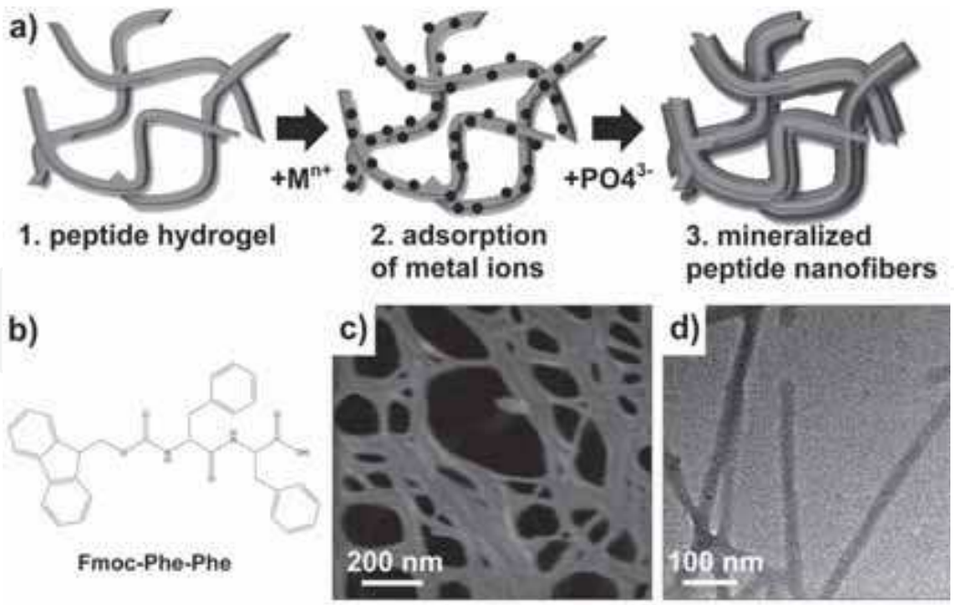

Fig. 22. Fabrication of peptide-amorphous $FePO_4$ hybrid material using the sequential injection method: (a) schematic diagram describing the fabrication process, (b) molecular structure of Fmoc-diphenylalaine, (c) SEM image and (d) TEM image of the peptide network (Ryu et al., 2010a).

Fe^{3+} ions, adsorbed during the Fe^{3+}-containing solution treatment, react with PO_4^{3-} during the injection of solution containing PO_4^{3-} to form a hybrid material of peptide template and electrochemically active amorphous $FePO_4$, as shown in Figure 23(a-b) (Ryu et al. 2010a). Interestingly, other transition metal phosphates also could be coated onto the peptide assembly by the same method as shown in Figure 23 (Ryu et al. 2010a).

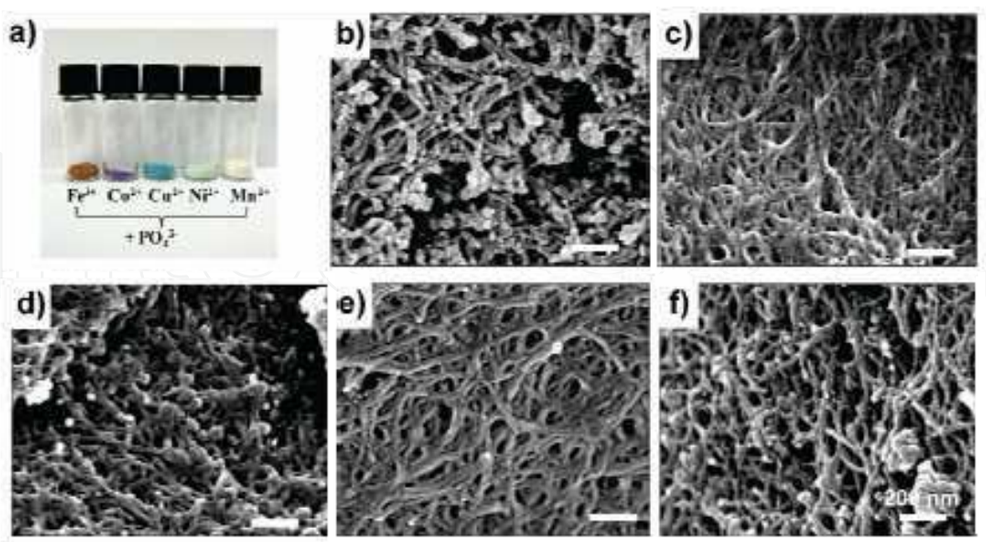

Fig. 23. (a) Photographs and (b-f) SEM images of various peptide-metal phosphate hybrid materials: injected metal ions are (b) Fe^{3+}, (c) Co^{2+}, (d) Cu^{2+}, (e) Ni^{2+} and (f) Mn^{2+} ions, respectively. (Ryu et al., 2010a).

The fabricated peptide-amorphous $FePO_4$ is annealed in adequate condition to remove the inactive peptide template, forming the amorphous $FePO_4$ nanotube, as illustrated in Figure 24(a) (Ryu et al. 2010a). Hollow space is formed inside the amorphous $FePO_4$, resulting in a nanotubular structure, as shown in Figure 24(c-d) (Ryu et al. 2010a). Another purpose for the heat treatment is to remove crystal water because it tends to form a hydrated phase of $FePO_4 \cdot 2H_2O$ when the $FePO_4$ phase is synthesized from aqueous solution. Heat treatment at too high temperature induces the crystallization of the amorphous phase, lowering the electrochemical activity (Okada et al., 2005). Thus, controlling the temperature is an important factor for the heat treatment. The individual nanotubes are interwoven with one another to form a complex network structure, as expected. The peptide leaves a thin amorphous carbon layer inside the tube after heat treatment, as which is identified by the FT-IR spectra shown in Figure 24(e) (Ryu et al. 2010a). Additionally, the FT-IR spectra confirm that the $FePO_4$ phase is successfully formed. The residual carbon layer is expected to provide a facile pathway for electron transport.

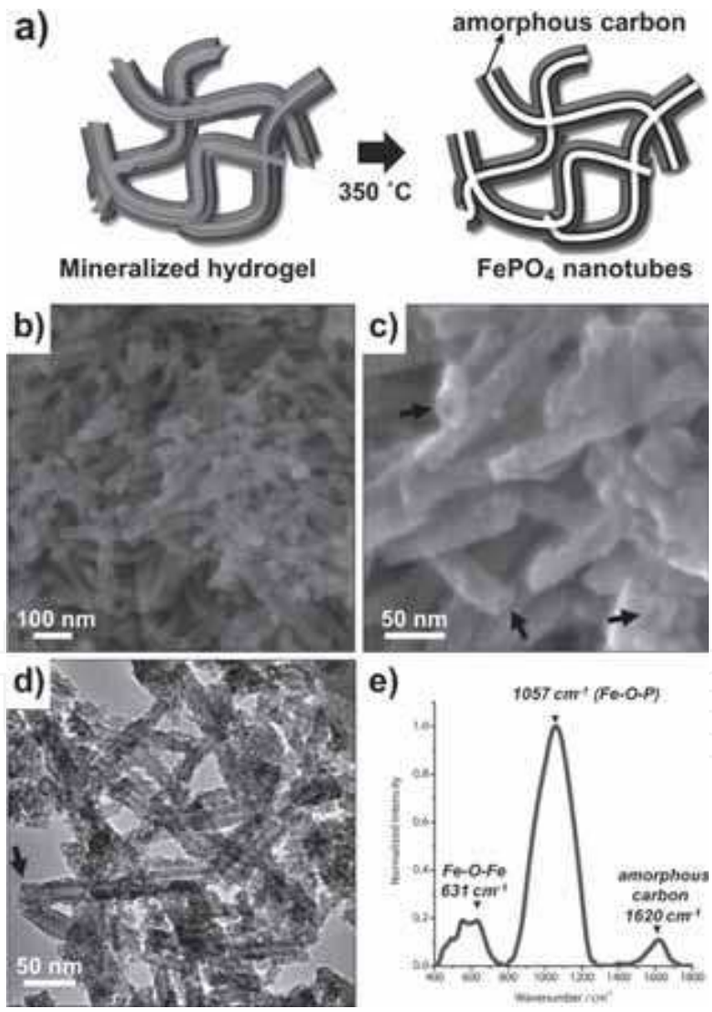

Fig. 24. Amorphous $FePO_4$ nanotube synthesized by a peptide template: (a) schematic diagram for synthesis procedure, (b-c) SEM images, (d) TEM image, and (e) FI-IR spectra (Ryu et al., 2010a).

As a cathode material, the amorphous $FePO_4$ nanotube coated by a carbon layer exhibits a high specific capacity, as depicted in Figure 25 (Ryu et al. 2010a). Its first discharge capacity is approximately 170 mAh g^{-1}, which is comparable to the theoretical capacity (178 mAh g^{-1}). Then, the specific capacity is saturated to 150 mAh g^{-1}, with excellent reversibility. Similar to the TiO_2 nanotube network, it is believed that the nanoscale dimension and unique nanostructure improve the electrochemical activity of amorphous $FePO_4$. The carbon layer inside the nanotube, which sufficiently supplies electrons for the electrochemical reaction, is also impressive.

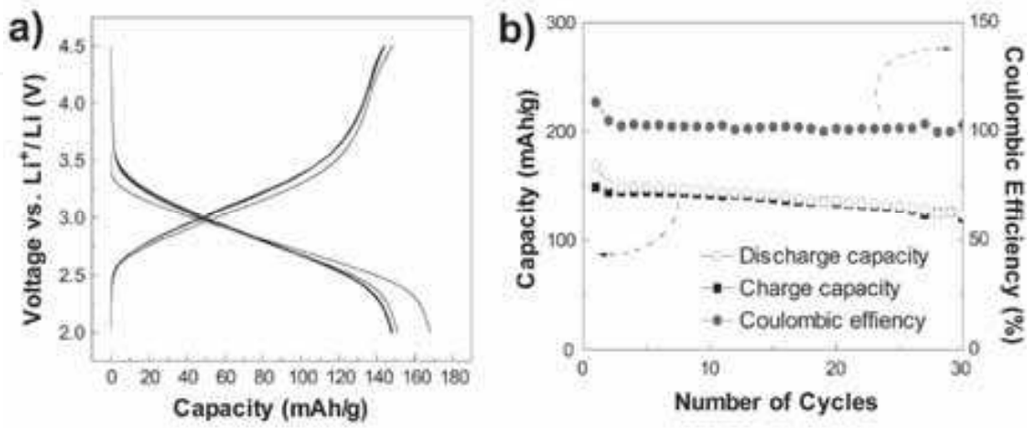

Fig. 25. (a) Discharge-charge profiles and (b) capacity retention of the amorphous $FePO_4$ nanotube at a current rate of 10 mA g^{-1} (Ryu et al., 2010a).

The morphology of the peptides is easily controllable because the self-assembly of the peptides is influenced simply by the assembly condition. Generally, peptides display numerous acidic and polar moieties on their surface. These moieties provide adsorption and nucleation sites for the electrode materials because they have high affinities for the ions or molecules forming the electrode materials. Various nanostructured electrode materials can be fabricated based on peptide assemblies. Among these, the network structure of hollow nanotubes is considered a high-performance structure. The unique nanostructure has advantages for battery performance, especially high-rate performance and capacity retention upon cycling. The two-directional Li-ion transport leads to improved Li-ion supply for the electrochemical reaction and the highly ordered nanotube network enhances cycle stability due to stress relaxation through the hollow and improved structural stability by interweaving. Furthermore, the anisotropic nanostructure is speculated to show faster electronic transport than the conventional isotropic nanostructure through one long dimension (Bruce et al., 2008). Although further investigation of the precise control of the peptide morphology and simple coating techniques is warranted, the strategy using the peptide assembly as the structural template is expected to be applied universally to fabricate various electrode materials with various nanostructures, and thus, to fabricate high performing Li rechargeable batteries.

4. Bio-inspired materials for other energy conversion devices

The synthesis and electrochemical characterization of the electrode materials based on virus and peptide templates for Li rechargeable batteries have been described in the above sections. In this section, the nanostructured materials based on the biomaterial templates for

other energy-conversion devices, such as solar cells and fuel cells, are discussed briefly. Solar cells and fuel cells generate electricity from sunlight and fuels such as H_2, respectively. As they generate the electricity whereas Li rechargeable batteries store the electricity, their combination can give rise to a new concept of energy device.

When a solar cell is exposed to sunlight, an electron-hole pair is generated by photons and simultaneously voltage and current are created. The solar cell is regarded as a most promising renewable green energy device due to the permanence of the sun. Among many types of solar cells, the Si-based quantum-dot solar cell is usually fabricated in the form of thin film, which typically requires a lithography process for structure determination. Here, biomaterials can be applied to the lithography process as a mask layer for etching (Huang et al., 2010). Ferritin, an Fe-containing protein, is assembled into a 2-D array on the SiO_2 surface. Shells of the protein are removed by heat treatment, leaving iron oxide cores for the mask. Following an adequate etching process, a 2-D array of the quantum-dot solar cells is successfully fabricated with 10-nm dimensions as shown in Figure 26 (Huang et al., 2010).

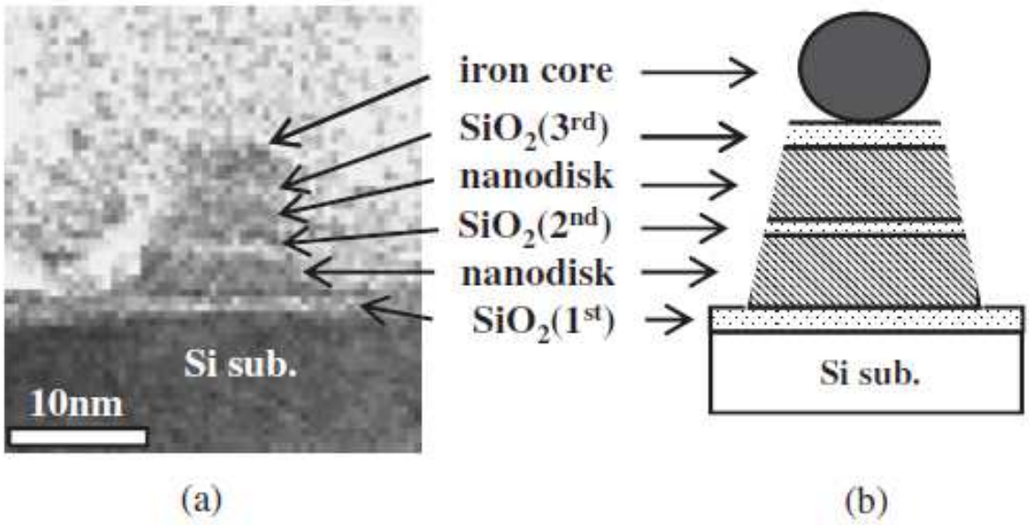

Fig. 26. (a) STEM image and (b) schematic diagram of a Si-based solar cell using ferritin protein as a mask layer (Huang et al., 2010).

Recently, dye-sensitized solar cells have attracted much interest due to their potentially lower production cost (Grätzel, 2005). Dye adsorbed onto a photo-anode generates electrons. The electrons are transferred to the photo-anode, generally TiO_2. Because the amount of dye adsorbed determines the solar-cell efficiency, a nanostructured photo-anode is required for a sufficiently high surface area to adsorb the dye. Figure 27 depicts the process for a nanostructured TiO_2 photo-anode based on a butterfly wing (Zhang et al., 2009). The butterfly-wing template is immersed in $Ti(SO_4)_2$ solution to sock the precursor solution. The socked template is placed on the TiO_2/FTO/glass substrate and then clamped tightly. The structurally duplicated TiO_2 photo-anode is prepared after a final heat treatment, as shown in Figure 28 (Zhang et al., 2009). The original honeycomb structure of the wing is well duplicated in the TiO_2 photo-anode. Its high surface area increases the amount of dye adsorbed. Furthermore, its unique nanostructure is advantageous for light absorption. As a result, the honeycomb structured TiO_2 photo-anode enhances the solar cell efficiency compared with that of conventional TiO_2 photo-anode without the butterfly-wing template.

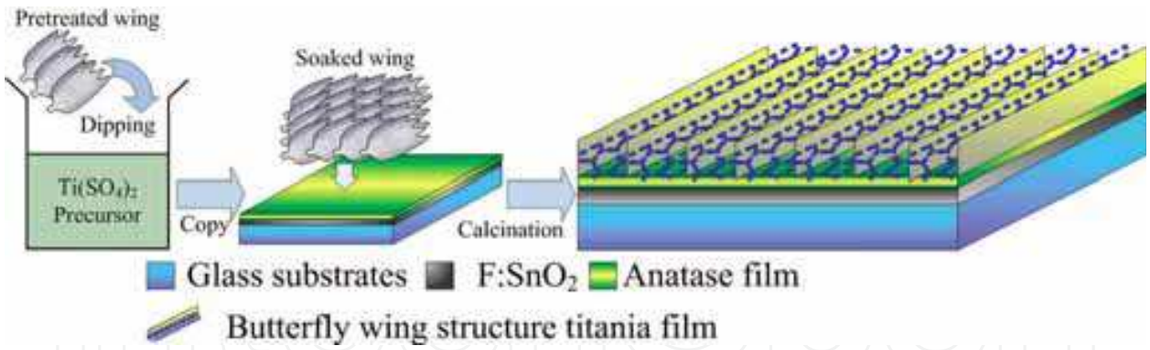

Fig. 27. Schematic diagram of the fabrication of a TiO_2 photo-anode based on butterfly-wing assembly (Zhang et al., 2009).

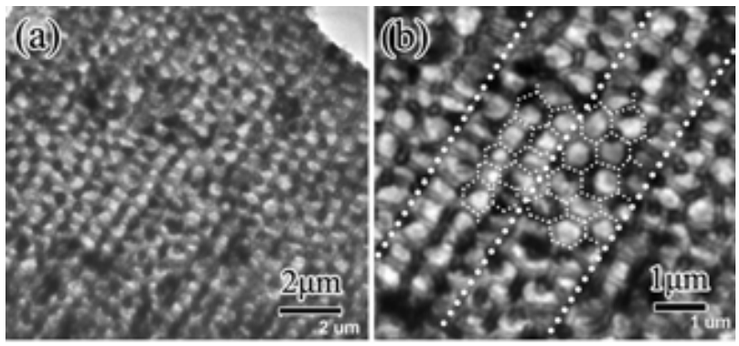

Fig. 28. TEM images of the butterfly wing-shaped TiO_2 photo-anode: (a) Medium resolution image and (b) high resolution image (Zhang et al., 2009).

Fuel cells generate electric energy from the oxidation of the fuel. For example, oxidation of H_2 generates the electric energy with the simultaneous reduction of O_2, leaving H_2O in a H_2-based fuel cell. When the fuel cell operates, a noble metal catalyst, such as Pt and Pd, is used to improve the oxidation efficiency, thereby increasing the output-energy density (Liu et al., 2006). Because the size and shape of the catalyst affect the oxidation efficiency significantly, nanostructure control of the catalyst is an important issue for a high-performance fuel cell. Bacteria are also adoptable as the template for the noble metal nucleation, as depicted Figure 29 (Yong et al., 2010). Pd nanoparticles are formed on the bacteria surface by sequential adsorption and reduction of Pd^{2+} ions. The particle size and homogeneity are influenced by the type of bacteria. The *D. desulfuricans*-Pd hybrid material shown in Figure 29(b) contains homogeneous small nanoparticles. The bacteria-Pd hybrid materials are sintered to serve as proton exchange membrane fuel cell catalysts. Furthermore, the fabrication of nanocatalysts with intermetallic compounds of noble metals is also possible. Compared to the commercial Pd catalyst, the catalyst fabricated based on the bacteria template shows enhanced power output. A similar outcome is achieved using tobacco mosaic virus (TMV) as the template, as shown in Figure 30 (Yong et al., 2010). TMV-Pt hybrid nanowires have been synthesized successfully with almost uniform individual size. The precursor concentration has a significant relationship with the size of the synthesized nanoparticles. As the catalyst for a fuel cell, the TMV-Pt hybrid nanowires exhibit better efficiency compared with simple Pt nanoparticles due to the increased electrochemically active surface area.

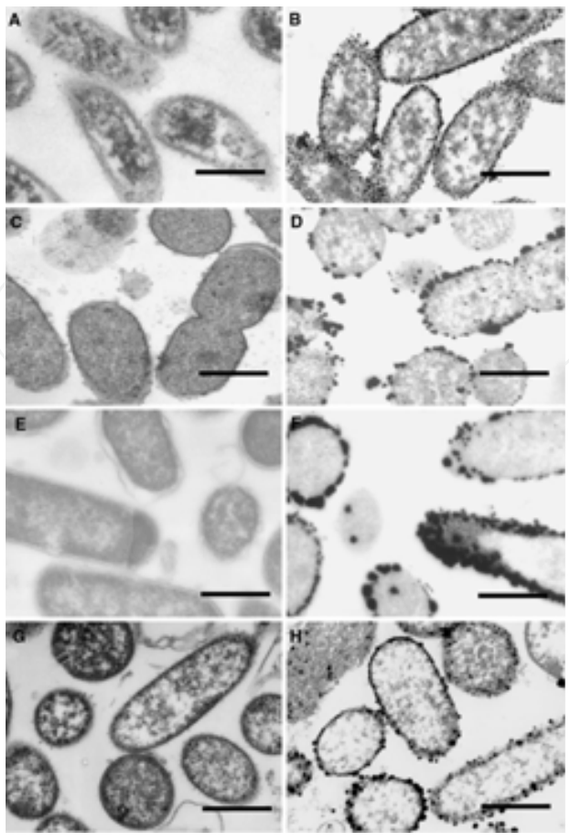

Fig. 29. TEM images of bacteria templates before (a, c, e, and g) and after (b, d, f, and h) the formation of Pd nanocatalyst: (a-b) *D. desulfuricans*, (c-d) *E. coli* MC4100, (e-f) *E. coli* IC007, and (g-h) *C. metallidurans* (Scale bar: 500 nm) (Yong et al., 2010).

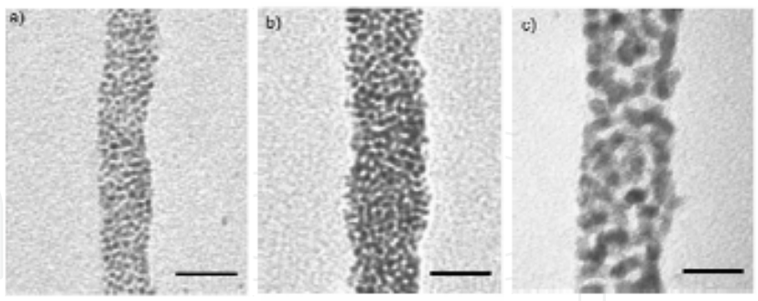

Fig. 30. TEM images of Pt-TMV hybrid nanowires prepared at various Pt precursor concentration. The concentrations increases from (a) through (c). (Scale bar: 20 nm) (Górzny et al., 2010).

5. Summary and perspective

In this chapter, the bio-inspired synthesis of electrode materials was briefly introduced for the application of next-generation Li rechargeable batteries. The use of self-assembled viruses and peptides as the templates for nanostructured electrode materials has been studied extensively. The electrode materials are coated onto the surface of the biomaterial

templates, making easily obtained isostructured electrode materials. The numbers of acidic and polar moieties at the surface of the biomaterials lead to high affinity of the coating electrode materials. The nanoarchitectures of biomaterials are easily controllable, and thus, the electrode materials can be varied by applying different structured biomaterial templates. The nanostructured electrode materials based on the biomaterial templates exhibit superior electrochemical performance, such as specific capacity, rate capability, and cyclability, due to the improved Li-ion and electron supply and the strain accommodation upon cycling.

Despite the potential of such bio-inspired syntheses, further research is required to realize their application in the Li rechargeable batteries. The electrode materials introduced in this chapter include the Co_3O_4 anode, TiO_2 anode, and amorphous $FePO_4$ cathode. More promising electrode materials should be tested. For example, amorphous $FePO_4$ has a severe drawback in that a Li-deficient phase is not preferred in the cathode. Conventional Li rechargeable batteries are composed of a Li-deficient anode and a Li-containing cathode. Therefore, investigations of the coating techniques for Li-containing cathode materials are needed. Additionally, the production cost of biomaterials such as peptides is relatively high for commercialization, and nanostructure formation with large-area uniformity is questionable from the perspective of mass production. Thus, it is necessary to investigate the technologies for controlling the morphology of biomaterial over a large area with reduced production costs.

Bio-inspired synthesis can generate various classes of materials, from metals to complex chemical compounds such as metal phosphates; thus, it represents a promising way to fabricate various kinds of devices, that require nanostructure materials for improved performance, as well as Li rechargeable batteries. Nature is the oracle that always inspires new developments by human beings for the a better life. Nature generates innumerable materials on the earth, and we only use some of them. Deep insight for material generation, not just from living organisms but from all products in nature, will present novel strategies with the opportunity to investigate materials for a better life.

6. Acknowledgment

This work was supported by a grant from the Fundamental R&D Program for Technology of World Premier Materials and Energy Resource Technology R&D Program (20092020100040) funded by the Ministry of Knowledge Economy, Republic of Korea. This work was also supported by the National Research Foundation of Korea Grant (R11-2008-058-01003-0, NRF-2009-0082069, NRF-2009-0094219) and Converging Research Center Program (2010K001088) funded by the Ministry of Education, Science, and Technology, Republic of Korea.

7. References

Bensaude-Vincent, B. ; Arribart, H. ; Bouligand, Y. & Sanchez, C. (2002). Chemists and The School of Nature, *New Journal of Chemistry*, Vol.26, No.1, (January 2002), pp. 1-5, ISSN 1144-0546

Sanchez, C.; Arribart, H. & Guille, M. M. G. (2005). Biomimetism and Bioinspiration as Tools for The Design of Innovative Materials and Systems, *Nature Materials*, Vol.4, No.4, (April 2005), pp.277-288, ISSN 1476-1122

Dickerson, M. B.; Sandhage, K. H. & Naik R. R. (2008). Protein- and Peptide-Directed Snytheses of Inorganic Materials, *Chemical Review*, Vol.108, No.11, (November 2008), pp. 4935-4978, ISSN 0009-2665

Lv, J.; Liu, H. & Li, Y. (2008). Self-Assembly and Properties of Low-Dimensional Nanomaterials Based on π-Conjugated Organic Molecules, *Pure and Applied Chemistry*, Vol.80, No.3, (March 2008), pp. 639-658, ISSN 0033-4545

Katz, E.; Willner, I. & Wang, J. (2004). Electroanalytical and Bioelectroanalytical Systems Based on Metal and Semiconductor Nanoparticles, *Electroanalysis*, Vol.16, No.1-2, (January 2004), pp. 19-44, ISSN 1040-0397

Su, H.; Han, J.; Dong, Q.; Zhang, D. & Guo, Q. (2008) *In Situ* Synthesis and Photoluminescence of QD-CdS on Silk Fibroin Fibers at Room Temperature, *Nanotechnology*, Vol.19, No.2, (January 2008), pp. 025601 , ISSN 0957-4484

Li, X.; Fan, T.; Zhou, H.; Chow, S.-K.; Zhang, W.; Zhang, D.; Guo, Q. & Ogawa, H. (2009) Enhanced Light-Harvesting and Photocatalytic Properties of *Morph*-TiO_2 from Green-Leaf Biotemplates, *Advanced Functional Materials*, Vol.19, No.1, (January 2009), pp. 45-56, ISSN 1616-301X

Moriarty, P. (2001), Nanostructured Materials, *Reports on Progress in Physics*, Vol.64, No.3, (March 2001), pp. 297-381, ISSN 0034-4885

Tarascon, J.-M. & Armand, M. (2001). Issues and Challenges Facing Rechargeable Lithium Batteries, *Nature*, Vol.414, No.6861, (November 2001), pp. 368-377, ISSN 0028-0836

Bruce, P. G.; Scrosati, B. & Tarascon, J.-M. (2008), Nanomaterials for Rechargeable Lithium Batteries, *Angewante Chemi International Edition*,Vol.47, No.16, (April 2008), pp. 2930-2946, ISSN 1433-7851

Kang, K.; Meng, Y. S.; Bréger, J.; Grey, C. P. & Ceder, G. (2006). Electrodes with High Power and High Capacity of Rechargeable Lithium Batteries, *Science*, Vol.311, No.5763, (February 2006), pp. 977-980, ISSN 0036-8075

Cheng, F.; Tao, Z.; Liang, J. & Chen. J. (2008). Template-Directed Materials for Rechargeable Lithium-Ion Batteries, *Chemistry of Materials*, Vol.20, No.3, (Febrary 2008), pp. 667-681, ISSN 0897-4756

Cui, H.; Webber, M. J. & Stupp, S. I. (2010). Self-Assembly of Peptide Amphiphiles: From Molecules to Nanostructures to Biomaterial, *Peptide Science*, Vol.94, No.1, (January 2010), pp. 1-18, ISSN 0006-3525

Ryu, J.; Kim, S.-W.; Kang, K. & Park, C. B. (2010a). Mineralization of Self-Assembled Peptide Nanofibers for Rechargeable Lithium Ion Batteries, *Advanced Materials*, Vol.22, No.48, (December 2010), pp. 5537-5541, ISSN 0935-9648

Reches, M. & Gazit, E. (2006). Molecular Self-Assembly of Peptide Nanostructures: Mechanism of Association and Potential Uses, *Current Nanoscience*, Vol.2, No.2, (May 2006), pp. 1573-4137, ISSN 1573-4137

Fraden, S. & Kamien, R. D. (2000). Self-Assembly in Vivo, *Biophysical Journal*, Vol.78, No.5, (May 2000), pp. 2189-2190, ISSN 0006-3495

Giese, C.; Demmler, C. D.; Ammer, R.; Hartmann, S.; Lubitz, A.; Muiiler, L.; Müller, R. & Marx, U. (2006). A Human Lymph Node in Vitro – Challenges and Progress, *Artificial Organs*, Vol.30, No.10, (October 2006), pp. 803-808, ISSN

Brachmann, C. B. & Cagan, R. L. (2003). Patterning the Fly Eye: The Role of Apotosis, *Trends in Genetics*, Vol.19, No.2, (February 2003), pp. 91-96, ISSN 0168-9525

Ryu, J. & Park, C. B. (2008). High-Temperature Self-Assembly of Peptides into Vertically Well-Aligned Nanowires by Aniline Vapor, *Advanced Materials*, Vol.20, No.19, (October 2008), pp. 3754-3758, ISSN 0935-9648

Xia, H.; Chan, H. S. O.; Xiao, C. & Cheng, D. (2004). Self-Assembled Oriented Conducting Polyaniline Nanotubes, *Nanotechnolgy*, Vol.15, No.12, (December 2004), pp. 1807-1811, ISSN 0957-4484

Zhou, H.; Fan, T. & Zhang, D. (2007). Hydrothermal Synthesis of ZnO Hollow Spheres Using Spherobacterium as Biotemplates, *Microporous and Mesoporous Materials*, Vol.100, No.1-3, (March 2007), pp. 322-327, ISSN 1387-1811

Zhang, T.; Wang, W.; Zhang, D.; Ma, Y.; Zhou, Y. & Qi, L. (2010). Biotemplated Synthesis of Gold Nanoparticle-Bacetria Cellulose Nanocomposites and Their Application in Biosensing, *Advanced Materials*, Vol.20, No.7, (April 2010), pp. 1152-1160, ISSN 0935-9648

Han, T. H.; Park, J. S.; Oh, J. K. & Kim, S. O. (2008). Morphology Control of One-Dimensional Peptide Nanostructures, *Journal of Nanoscience and Nanotechnology*, Vol.8, No.10, (October 2010), pp. 5547-5550, ISSN 1550-7033

Lee, S.-W.; Lee, S. K. & Belcher, A. M. (2003). Virus-Based Alignment of Inorganic, Organic, and Biological Nanosized Materials, *Advanced Materials*, Vol.15, No.9, (May 2003), pp. 689-692, ISSN 0935-9648

Nam, K. T.; Peele, B. R.; Lee, S.-W. & Belcher, A. M. (2004). Genetically Driven Assembly of Nanorings Based on the M13 Virus, *Nano Letters*, Vol.4, No.1, (January 2004), pp. 23-27, ISSN 1530-6984

Mao, C.; Flynn, C. E.; Hayhurst, A.; Sweeney, R.; Georgiou, G.; Iverson, B. & Belcher, A. M. (2003). Viral Assembly of Oriented Quantum Dot Nanowires, *Proceedings of the National Academy of Sciences*, Vol.100, No.12, (June 2003), pp. 6946-6951, ISSN 0027-8424

Lee, Y. J.; Yi, H.; Kim, W.-J.; Kang, K.; Yun, D. S.; Strano, M. S.; Ceder, G. & Belcher, A. M. (2009). Fabricating Genetically Engineered High-Power Lithium-Ion Batteries Using Multiple Virus Genes, *Science*, Vol.324, No.5390, (May 2009), pp. 1051-1055, ISSN 0036-8075

Okada, S.; Tamamoto, T.; Okazaki, Y.; Yamiaki, J.; Tokunaga, M. & Nishida, T. (2005) Cathode Properties of Amorphous and Crystalline $FePO_4$, *Journal of Power Sources*, Vol.146, No.1-2, (August 2005), pp. 570-574, ISSN 0378-7753

Kang, Y.-M.; Song, M.-S.; Kim, J.-H.; Kim, H.-S.; Park, M.-S.; Lee, J.-Y.; Liu, H. K. & Dou, S. X. (2005). A Study on The Charge-Discharge Mechanism of Co_3O_4 as an Anode for The Li Ion Secondary Battery, *Electrochimica Acta*, Vol.50, No.18, (June 2005), pp. 3667-3673

Li, Y.; Tan, B. & Wu, Y. (2008), Mesoporous Co_3O_4 Nanowire Array for Lithium Ion Battery with High Capacity and Rate Capability, *Nano Letters*, Vol.8, No.1, (January 2008), pp. 265-270, ISSN 1530-6984

Nam, K. T.; Kim, D.-W.; Yoo, P. J.; Chiang, C.-Y.; Meethong, N.; Hammond, P. T.; Chiang, Y.-M. & Belcher, A. M. (2008). Virus-Enabled Synthesis and Assembly of Nanowires for Lithium Ion Battery Electrodes, *Science*, Vol.312, No.5775, (May 2006), pp. 885-888, ISSN 0036-8075

Nam, K. T.; Wartena, R.; Yoo, P. J.; Liau, F. W.; Chiang, Y.-M.; Hammond, P. T. & Belcher, A. M. (2008). Stamped Microbattery Electrode Based on Self-Assembled M13 Viruses, *Proceedings of the National Academy of Sciences*, Vol.105, No.45, (November 2008), pp. 17227-17231, ISSN 0027-8424

Huang, Y.; Chiang, C.-Y.; Lee, S. K.; Gao, Y.; Hu, E. L.; Yoreo, J. D. & Belcher, A. M. (2005). Programmable Assembly of Nanoarchitectures Using Genetically Engineered Viruses, *Nano Letters*, Vol.5, No.7, (July 2005), pp. 1429-1434, ISSN 1530-6984

Stoker, H. S. (2010). Proteins, In: *General, Organic, and Biological Chemistry*, Kilean Kennedy, (Ed.), pp. 655-697, Brooks Cole, ISBN 978-054-7152-81-3, California, USA

Ryu, J.; Kim, S.-W.; Kang, K. & Park, C. B. (2010b). Synthesis of Diphenylalanine/Cobalt Oxide Hybrid Nanowires and Their Application to Energy Storage, *ACS Nano*, Vol.4, No.1, (January 2010), pp. 159-164, ISSN 1936-0851

Kim, S.-W.; Han, T. H.; Kim, J.; Gwon, H.; Moon, H.-S.; Kang, S.-W.; Kim, S. O. & Kang, K. (2009). Fabrication and Electrochemical Characterization of TiO_2 Three-Dimensional Nanonetwork Based on Peptide Assembly, *ACS Nano*, Vol.3, No.5, (May 2009), pp. 159-164, ISSN 1936-0851

Kim, S.-W.; Kwon, S.-H.; Jeong, S.-J. & Kang, S.-W. (2008). Improvement of Copper Diffusion Barrier Properties of Tantalum Nitride Films by Incorporating Ruthenium using PEALD, *Journal of The Electrochemical Society*, Vol.155, No.11, (September 2008), pp. H885-H888, ISSN 0013-4651

Zhao, Y.; Wei, M.; Lu, Jun.; Wang, Z. L. & Duan, X. (2009). Biotemplated Hierarchical Nanostructure of Layered Double Hydroxides with Improved Photocatalysis Performance, *Nano Letters*, Vol.3, No.12, (December 2009), pp. 4009-4016, ISSN 1530-6984

Geroge, S. M. (2010). Atomic Layer Deposition: An Overview, *Chemical Reviews*, Vol.110, No.1, (January 2010), pp. 111-131, ISSN 0009-2665

Xu, J.; Wang, Y.; Li, Z. & Zhang, W. F. (2008). Preparation and Electrochemical Properties of Carbon-Doped TiO_2 Nanotubes as an Anode Material for Lithium-Ion Batteries, *Journal of Power Sources*, Vol.175, No.2, (January 2008), pp. 903-908, ISSN 0378-7753

Wagemaker, M.; Borghols, W. J. H. & Mulder, F. M. (2007). Large Impact of Particle Size on Insertion Reactions. A Case for Anatase Li_xTiO_2, *Journal of The American Chemical Society*, Vol.129, No.14, (April 2007), pp. 4323-4327, ISSN 0002-7863

Huang, C.-H.; Igarashi, M.; Horita, S.; Takeguchi, M.; Uraoka, Y.; Fuyuki, T.; Yamashita, I. & Samukawa, S. (2010). Novel Si Nanodisk Fabricated by Biotemplate and Defect-Free Neutral Beam Etching for Solar Cell Application, *Japanese Journal of Appliced Physics*, Vol.49, No.4, (April 2010), pp. 04DL16, ISSN 0021-4922

Grätzel, M. (2005). Solar Energy Conversion by Dye-Sensitized Photovoltaic Cells, *Inorganic Chemistry*, Vol.44, No.20 (October 2005), pp. 6841-6851, ISSN 0020-1669

Zhang, W.; Zhang, D.; Fan, T.; Gu, J.; Ding, J.; Wang, H.; Guo, Q. & Ogawa, H. (2009). Novel Photoanode Structure Templated from Butterfly Wing Scales, *Chemistry of Materials*, Vol.21, No.1, (January 2009), pp. 33-40, ISSN 0897-4756

Liu, H.; Song, C.; Zhang, L.; Zhang, J. ; Wang, H. & Wilkinson, D. P. (2006). A Review of Anode Catalysis in The Direct Methanol Fuel Cell, *Journal of Power Sources*, Vol.155, No.2, (April 2006), pp. 95-110, ISSN 0378-7753

Yong, P.; Mikheenko, I. P.; Deplanche, K.; Redwood, M. D. & Macaskie, L. E. (2010). Biorefining of Precious Metals from Wastes: An Answer to Manufacturing of Cheap Nanocatalyst for Fuel Cells and Power Generation via and Integrated Biorefinery?, *Biotechnology Letters*, Vol.32, No.12, (December 2010), pp. 1821-1828, ISSN 0141-5492

Górzny, M. L.; Walton, A. S. & Evans, S. D. (2010). Synthesis of High-Surface-Area Platinum Nanotubes Using a Viral Template, *Advanced Functional Materials*, Vol.20, No.8, (April 2010), pp. 1295-1300, ISSN 1616-301X

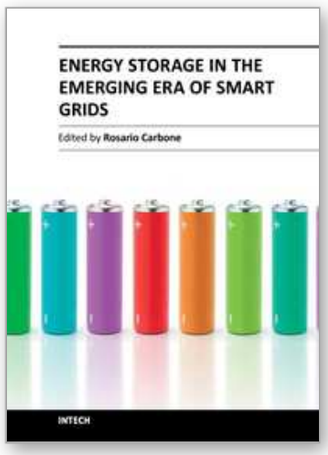

Energy Storage in the Emerging Era of Smart Grids

Edited by Prof. Rosario Carbone

ISBN 978-953-307-269-2
Hard cover, 478 pages
Publisher InTech
Published online 22, September, 2011
Published in print edition September, 2011

Reliable, high-efficient and cost-effective energy storage systems can undoubtedly play a crucial role for a large-scale integration on power systems of the emerging â€œdistributed generationâ€ (DG) and for enabling the starting and the consolidation of the new era of so called smart-grids. A non exhaustive list of benefits of the energy storage properly located on modern power systems with DG could be as follows: it can increase voltage control, frequency control and stability of power systems, it can reduce outages, it can allow the reduction of spinning reserves to meet peak power demands, it can reduce congestion on the transmission and distributions grids, it can release the stored energy when energy is most needed and expensive, it can improve power quality or service reliability for customers with high value processes or critical operations and so on. The main goal of the book is to give a date overview on: (I) basic and well proven energy storage systems, (II) recent advances on technologies for improving the effectiveness of energy storage devices, (III) practical applications of energy storage, in the emerging era of smart grids.

How to reference

In order to correctly reference this scholarly work, feel free to copy and paste the following:

Kisuk Kang and Sung-Wook Kim (2011). Bio-Inspired Synthesis of Electrode Materials for Lithium Rechargeable Batteries, Energy Storage in the Emerging Era of Smart Grids, Prof. Rosario Carbone (Ed.), ISBN: 978-953-307-269-2, InTech, Available from: http://www.intechopen.com/books/energy-storage-in-the-emerging-era-of-smart-grids/bio-inspired-synthesis-of-electrode-materials-for-lithium-rechargeable-batteries

INTECH
open science | open minds

InTech Europe
University Campus STeP Ri
Slavka Krautzeka 83/A
51000 Rijeka, Croatia
Phone: +385 (51) 770 447
Fax: +385 (51) 686 166
www.intechopen.com

InTech China
Unit 405, Office Block, Hotel Equatorial Shanghai
No.65, Yan An Road (West), Shanghai, 200040, China
中国上海市延安西路65号上海国际贵都大饭店办公楼405单元
Phone: +86-21-62489820
Fax: +86-21-62489821

IntechOpen